UMEÅ UNIVERSITY

The fW-mean Filter Framework for Topology Optimization and Analysis of Friedrichs Systems

Linus Hägg

Doctoral thesis, 2020
Department of Computing Science, Umeå University

Department of Computing Science, Umeå University
SE–901 87 Umeå, Sweden
www.cs.umu.se

ISBN: 978-91-7855-367-9 (print)
ISBN: 978-91-7855-368-6 (digital)
ISSN: 0348-0542
UMINF 20.09
Electronic version available at http://umu.diva-portal.org/
Printed by: CityPrint i Norr AB
Umeå, Sweden 2020

Acknowledgments

First, I want to thank my supervisors Martin Berggren and Eddie Wadbro for your endless commitment in my doctoral education—I have been truly fortunate in this respect. Martin, I really enjoyed the enlightening discussions we had at the white-board, or over some *ärtsoppa och plättar*[1] in the lunch restaurant. I am also grateful that you made it possible, and encouraged me to partake in scientific events abroad. Eddie, it is with joy I remember the many discussions we had early in the morning over a cup of coffee or tea in the UMIT lounge while sorting out the fW-mean filter framework.

I would like to express my deepest gratitude to Professor Rainer Picard for many interesting discussions and suggestions on how to tackle the *dreadful drift term*.

I thank current and former members of the Design Optimization group for reviewing and commenting my work, and my colleagues at the UMIT research lab, the department of Computing Science, and RISE Research Institutes of Sweden for providing a pleasant and friendly working environment.

I also gratefully acknowledge the financial support from the Swedish Research Council (grant numbers 2013-03706 and 2018-03546), and eSSENCE, a strategic collaborative eScience program funded by the Swedish Research Council.

Finally, I want to thank my family, which I will do in Swedish. När jag tänker efter har det nog varit rätt uppenbart redan från tidiga år att jag skulle bli forskare. Jag minns hur jag som skolbarn satt vid skrivbordet i mormor och morfars kontor och knappade på en miniräknare. Med hjälp av formler som jag letat fram i uppslagsverket som stod i bokhyllan och ett närmevärde till π (pi), med så många decimaler som rymdes på miniräknarens display, räknade jag ut cirklars areor och omkretsar. Döm av min förvåning och upphetsning när jag efter en stund upptäckte att kvoten mellan arean och omkretsen i kvadrat alltid gav samma värde, oavsett vilken radie jag använde! Rusig av upptäckten gick jag vidare till andra former så som kvadrater och hexagoner och fann liknande samband med hjälp av miniräknaren och formler från uppslagsverket. Min familj har på olika sätt och vid olika tidpunkter i mitt liv uppmuntrat och väckt mitt intresse för matematik, naturvetenskap och teknik, vilket jag är oändligt tacksam för.

Lovisa, *med dig vid min sida klarar jag allt*. Utan ditt stöd hade jag aldrig lyckats färdigställa denna avhandling, tack.

Harry och Solveig, i ärlighetens namn är ert bidrag till min doktorsavhandling rätt litet, eller till och med obefintligt, men till livet desto större.

Linus Hägg
Skellefteå 2020

[1] pea soup and pancakes

Abstract

Part I. Topology optimization is the most general form of design optimization in which the optimal layout of material within a given region of space is to be determined. Filters are essential components of many successful density based topology optimization approaches. The generalized fW-mean filter framework developed in this thesis provides a unified platform for construction, analysis, and implementation of filters. Extending existing algorithms, we demonstrate that under special albeit relevant conditions, the computational complexity of evaluating generalized fW-mean filters and their derivatives is linear in the number of design degrees of freedom. We prove that generalized fW-mean filters guarantee existence of solutions to the penalized minimum compliance problem, the archetypical problem in density based topology optimization. In this problem, the layout of linearly elastic material that minimizes the compliance given static supports and loads is to be determined. We formalize the connection between mathematical morphology and the notion of minimum length scale of a layout of material and thereby provide a theoretical foundation for imposing and assessing minimum length scales in density based topology optimization. Elaborating on the fact that some sequences of generalized fW-mean filters provide differentiable approximations of morphological operators, we devise a method capable of imposing different minimum length scales on the two material phases in minimum compliance problems.

Part II. The notion of Friedrichs systems, also known as symmetric positive systems, encompasses many linear models of physical phenomena. The prototype model is Maxwell's equations, which describe the evolution of the electromagnetic field in the presence of electrical charges and currents. In this thesis, we develop well-posed variational formulations of boundary and initial–boundary value problems of Friedrichs systems on bounded domains. In particular, we consider an inhomogeneous initial–boundary value problem that models lossless propagation of acoustic disturbances in a stagnant fluid. Galbrun's equation is a linear second order vector differential equation in the so-called Lagrangian displacement, which was derived to model lossless propagation of acoustic disturbances in the presence of a background flow. Our analysis of Galbrun's equation is centered on the observation that solutions to Galbrun's equation may be formally constructed from solutions to linearized Euler's equations. More precisely, the Lagrangian displacement is constructed as the solution to a transport-type equation driven by the Eulerian velocity perturbation. We present partial results on the well-posedness of Galbrun's equation in the particular case that the background flow is everywhere tangential to the domain boundary by demonstrating mild well-posedness of an initial–boundary value problem for linearized Euler's equations and that our construction of the Lagrangian displacement is well-defined. Moreover, we demonstrate that sufficiently regular solutions to Galbrun's equation satisfy an energy estimate.

Populärvetenskaplig sammanfattning

Del 1. Målet med topologioptimering är att bestämma den bästa utformningen av ett givet material. Ett klassiskt exempel, illustrerat i Figur 1a, går ut på att från en given mängd stål utforma en så styv konsolbalk som möjligt.

Ett möjligt, men mycket resurskrävande, tillvägagångssätt för att hitta en ”bra” utformning är att tillverka en stor uppsättning konsolbalkar av rätt mängd stål, men med olika utformningar, och sedan experimentellt bestämma vilken som är bäst, det vill säga styvast. Processen kan sedan upprepas med en ny uppsättning konsolbalkar, som utformats med utgångspunkt i föregående omgångs vinnande utformning, tills det att prestandan är tillfredställande eller att resurserna tagit slut.

En annan möjlighet är att nyttja matematiska beräkningsmodeller och datorsimuleringar för att utvärdera virtuella utformningar av konsolbalkar. Ännu bättre blir det om vi inte bara använder den matematiska modellen till att utvärdera virtuella utformningar, utan även till att systematisk föreslå prestationsförbättrande förändringar av givna virtuella utformningar. Denna virtuella designprocess som innefattar matematiska beräkningsmodeller, optimeringsalgoritmer och datorsimuleringar kan kallas beräkningsbaserad konstruktionsoptimering.

Innan konsolbalkens utformning kan optimeras av en dator med begränsade resurser måste problemet diskretiseras, så att antalet upptänkliga utformningar begränsas. Antalet utformningar begränsas vanligen genom att det grå området i Figur 1a indelas i ett rutnät med ändligt antal rutor som antingen kan innehålla stål eller vara tomma, så som illustreras i Figurerna 1b och 1c. Målet med optimeringen blir då helt enkelt att bestämma vilka rutor som ska innehålla stål och vilka som ska vara tomma.

Vad händer då om rutnätet förfinas? Jo, antalet upptänkliga utformningar växer mycket snabbt med antalet rutor i rutnätet. Och allt som oftast konvergerar inte den

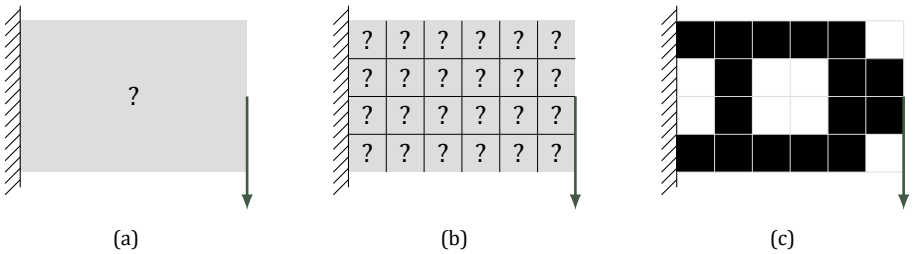

Figur 1: (a) I vårt exempel efterfrågas den optimala utformningen av en konsolbalk som är fäst vid en vägg i ena änden och belastad i motstående ände. (b) För att kunna optimera konsolbalkens utformning med hjälp av en dator, diskretiseras problemet med hjälp av ett rutnät så att målet med optimeringen blir att bestämma vilka rutor som skall innehålla stål. (c) Exempel på utformning av en konsolbalk där rutor innehållande stål svartfärgats.

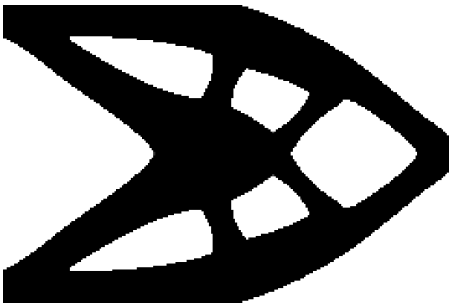

$240 \times 160 = 38\,400$ rutor

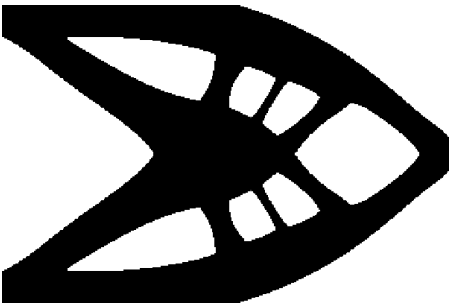

$360 \times 240 = 86\,400$ rutor

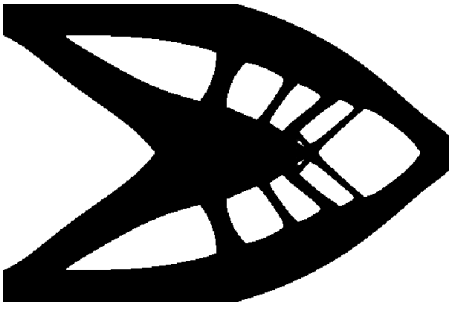

$480 \times 320 = 153\,600$ rutor

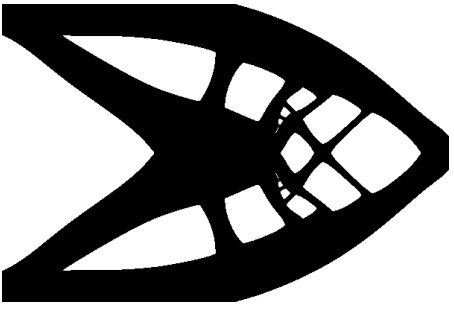

$600 \times 400 = 240\,000$ rutor

Figur 2: En följd konsolbalksutformningar som optimerats med samma förutsättningar men med allt finare rutnät. Som tidigare indikeras stål av svartfärgade rutor. Notera särskilt att finare rutnät leder till att det uppkommer fler och mindre detaljer i den optimerade utformningen.

optimerade utformningen, utan varje förfining av rutnätet leder till uppkomsten av finare strukturer och urtag, så som illustreras i Figur 2.

Bristen på konvergens belyser ett fundamentalt problem med den ursprungliga formuleringen av optimeringsproblemet, nämligen att det saknas lösningar. Situationen är inte helt olik den som uppstår när man ställer upp problemet:

(i) *Vilket är det minsta talet på tallinjen som är större än* 0*?*

Svaret är att det inte finns något sådant tal, eftersom det givet ett tal som är större än 0 alltid går att hitta ett mindre—det är bara att ta talet som ligger mittemellan 0 och det givna talet på tallinjen. På fackspråk säger man att problemet är felställt. För att komma vidare måste vi helt enkelt omformulera problemet. Vi har i huvudsak att välja mellan följande formuleringar:

(ii) *Vilket är det minsta talet på tallinjen som är större än eller lika med* 0*?*

(iii) *Vilket är det minsta talet på tallinjen som är större än eller lika med* 1*?*

Notera att valet av talet 1 i formulering (iii) är helt godtyckligt, men ju mindre tal (större än 0) vi väljer, desto närmre kommer vi den ursprungliga formuleringen (i). Formulering (ii) är en så kallad *relaxering* av den ursprungliga formuleringen (i),

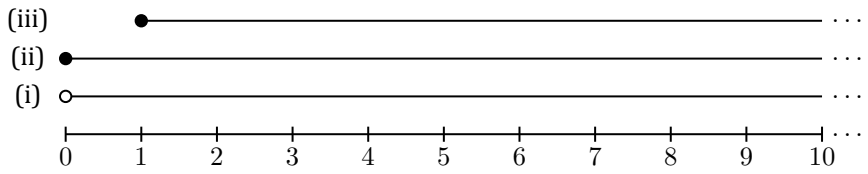

Figur 3: Illustration av de tre formuleringarnas mängder av möjliga lösningar. Fylld cirkel indikerar att ändpunkten ingår, ofylld att den ej ingår. Formulering (ii) är en relaxering av formulering (i) medan formulering (iii) är en restriktion.

medan formulering (iii) är en *restriktion*. Vid relaxering utvidgas mängden i vilken lösningen söks, medan restriktionen innebär att mängden av möjliga lösningar istället begränsas. Figur 3 visar grafiskt hur de tre formuleringarnas mängder av möjliga lösningar förhåller sig till varandra. Vi finner att lösningen till formulering (ii) är 0, vilken *inte* ingår i den ursprungliga formuleringens mängd av möjliga lösningar. Lösningen till formulering (iii) är 1, vilken ingår i den ursprungliga formuleringens mängd av möjliga lösningar. I det här enkla exemplet spelar det kanske inte så stor roll att 0 inte ingår i den ursprungliga mängden av möjliga lösningar, men i vårt konsolbalksoptimeringsproblem skulle en relaxering resultera i att mängden av möjliga lösningar utökas med utformningar som är i det närmaste omöjliga att tillverka eftersom de innehåller mikrostrukturer. Vi väljer därför att göra en restriktion av konsolbalksoptimeringsproblemet genom att introducera ett filter, vars roll är att begränsa mängden upptänkliga utformningar.

I denna avhandling används filter som härmar så kallade morfologiska operatorer som först utvecklades för bildbehandling. Dessa begränsar hur små strukturer och urtag som tillåts i konsolbalkarna oberoende av rutornas storlek. På så sätt förhindras uppkomsten av för små strukturer eller urtag när rutnätet förfinas. Användningen av filter som härmar morfologiska operatorer kan liknas vid effekten av att endast använda pennor med en viss storlek för att rita utformningarna. Pennstorleken kontrollerar utformningarnas detaljrikedom—en tunn penna kan rita finare detaljer än vad en tjock penna kan. Dock leder en begränsning av antalet detaljer, det vill säga en större penna i vår liknelse, till sämre prestanda i form av minskad styvhet vilket illustreras i Figur 4. För topologioptimeringsproblem finns det alltså anledning att

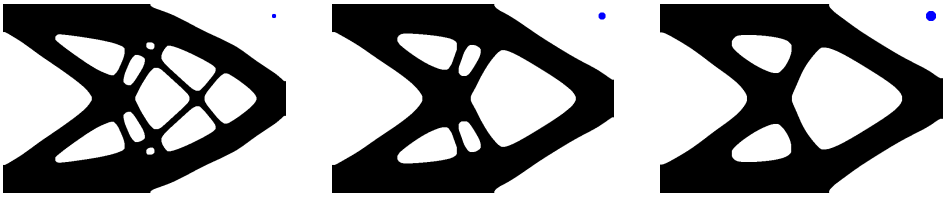

Figur 4: Konsolbalksutformningar som optimerats med $768 \times 512 = 393\,216$ rutor och filter som härmar morfologiska operatorer. De blå cirkelskivorna indikerar den minsta storleken på strukturer och urtag som tillåts av filtren. Styvheten anges relativt den vänstra utformningens styvhet.

väga utformningarnas prestanda mot deras komplexitet vid valet av ”penna”, det vill säga filter.

I avhandlingens första del introduceras ramverket för generaliserade fW-medelvärdesfilter, som erbjuder en plattform för enhetlig analys av såväl nya som en majoritet av redan existerande filter. Nedan presenteras ett urval av resultaten från avhandlingens första del.

- Vi ger ett matematiskt bevis för att restriktionen med hjälp av generaliserade fW-medelvärdesfilter av konsolbalksoptimeringsproblemet och liknande topologioptimeringsproblem är lösbara.
- Vi presenterar och utvecklar beräkningseffektiva filtreringsalgoritmer för generaliserade fW-medelsvärdesfilter som är lämpade för storskaliga topologioptimeringsproblem.
- Vi klargör kopplingen mellan morfologiska operatorer och den minsta storleken på en utformning.
- Vi presenterar en metod för konsolbalksoptimeringsproblemet och liknande topologioptimeringsproblem som oberoende begränsar de minsta storlekarna på strukturer *och* urtag i utformningarna med hjälp av generaliserade fW-medelvärdesfilter som härmar morfologiska operatorer.
- Vi demonstrerar användbarheten av ramverket för generaliserade fW-medelvärdesfilter i utmanande, realistiska problem genom att utveckla en filterstrategi för topologioptimering av en koaxial-vågledar-övergång.

Del 2. I del 1 stötte vi på begreppet felställt problem som naturligt väcker frågan om vad som är ett *rättställt* problem? Enligt Jaques Hadamard, som introducerade begreppet rättställdhet i början av nittonhundratalet, är ett problem rättställt om det finns en unik lösning som inte ändras oberäkneligt vid små förändringar av förutsättningarna (problemformuleringen). Den typ av problem vi har i åtanke i del 2 handlar om att förutspå fysikaliska skeenden från givna förutsättningar. Den del av Hadamards karaktärisering av rättställdhet som handlar om lösningens känslighet, påverkar möjligheten att noggrant lösa problemet med hjälp av en dator. Innan problemet kan lösas med hjälp av en dator med ändliga resurser måste det diskretiseras, precis som i fallet med konsolbalksoptimeringsproblemet. Det diskreta problemet är oftast lösbart, men diskretiseringen innebär nästan oundvikligen att förutsättningarna (problemformuleringen) ändras, så om det ursprungliga problemet inte är rättställt, är det troligt att den beräknade lösningen är mer eller mindre oanvändbar. Det är därför önskvärt att, om möjligt, försäkra sig om att problemet är rättställt innan det diskretiseras och löses med hjälp av en dator.

Många ekvationer som beskriver fysikaliska skeenden kan formuleras som så kallade Friedrichssystem. Som exempel kan nämnas Maxwells ekvationer som beskriver det elektromagnetiska fältet, eller ekvationerna som beskriver ljudutbredning i luft. Ljud består som bekant av förtunningar och förtätningar som propagerar genom luften. Oftast antas att ljudutbredningen sker i stillastående luft, men den som lyssnat på en utomhuskonsert i byiga vindar har säkerligen inte undgått att notera vindens påverkan på ljudet. I början av 1930-talet formulerade fransmannen Henri

Galbrun en ekvation som modellerar ljudutbredningen med hänsyn till vinden, till exempel vid utomhuskonserter eller i närheten av flygplan eller vindkraftverk. Det är intressant att veta att Galbruns ekvation även tillämpas på något så utomjordiskt som vågrörelser i solen.

Galbruns ekvation, som egentligen utgörs av ett system av tre ekvationer, härleds från Eulers sex ekvationer, som beskriver vätskor och gasers rörelser. Som standardalternativ till Galbruns ekvation finns lineariserade Eulers ekvationer. Det finns, förutom reduceringen från sex till tre ekvationer, ett antal skäl till att Galbruns ekvation är intressant. Ett är att lösning av Galbruns ekvation inte direkt ger oss ljudfältet, utan det så kallade Lagrangeiska förskjutningsfältet, från vilket alla delar av ljudfältet kan beräknas. Ett annat skäl är att formuleringen i det Lagrangeiska förskjutningsfältet förenklar hanteringen av randvillkor. Randvillkor är sådana villkor som lösningen måste uppfylla vid de ytor, även kallade ränder, som begränsar beräkningsområdet. Vissa randvillkor är av fysisk karaktär, till exempel vid väggar, golv och tak i ett rum som reflekterar ljudet, medan andra är mer artificiella, till exempel de som sätts i en dörröppning där man antar att ljudet obehindrat kan passera ut ur rummet utan att reflekteras. Syftet med de artificiella ränderna är att begränsa beräkningsområdet och därigenom beräkningskostnaden. För Friedrichssystem i allmänhet är hanteringen av randvillkor komplicerad. Några allmänna resultat angående rättställdheten av Galbruns ekvation finns inte i den vetenskapliga litteraturen, och de resultat som finns berör i huvudsak olika utvidgningar där ekvationen modifierats. Känt är dock att naiva försök att diskretisera och sedan lösa Galbruns ekvation med hjälp av en dator har misslyckats.

Den andra delen av denna avhandling analyserar rättställdhet för ett antal Friedrichssystem, i synnerhet system som modellerar ljudutbredning. Nedan presenteras ett urval av resultaten från andra delen.

- Vi utvecklar rättställda variationsformuleringar[2] för tre olika exempel på Friedrichssystem, bland andra ett system som modellerar ljudutbredning i stilla luft.

- Vi presenterar en alternativ härledning av Galbruns ekvation, i vilken det Lagrangeiska förskjutningsfältet definieras från en lösning till lineariserade Eulers ekvationer. Härledningen belyser på så sätt möjligheten att konstruera lösningar till Galbruns ekvation från lösningar till lineariserade Eulers ekvationer.

- Vi presenterar delresultat angående rättställdheten av Galbruns ekvation i fallet då vinden inte korsar beräkningsområdets ränder, genom att visa att lineariserade Eulers ekvationer är rättställda och att vår konstruktion av det Lagrangeiska förskjutningsfältet är väldefinierad.

[2] Variationsformuleringar används ofta för att generera diskretiseringar som lämpas för lösning med hjälp av datorer.

List of publications

As indicated in the title, this thesis is divided into two parts dedicated to *The fW-mean Filter Framework for Topology Optimization* and *Analysis of Friedrichs Systems*, respectively.

Part I is based on the following publications

I Eddie Wadbro and Linus Hägg, *On quasi-arithmetic mean based filters and their fast evaluation for large-scale topology optimization*. Structural and Multidisciplinary Optimization, 52(5), 879–888, 2015

II Linus Hägg and Eddie Wadbro, *Nonlinear filters in topology optimization: Existence of solutions and efficient implementation for minimal compliance problems.* Structural and Multidisciplinary Optimization, 55(3), 1017-1028, 2017

III Linus Hägg and Eddie Wadbro, *On minimum length scale control in density based topology optimization.* Structural and Multidisciplinary Optimization, 58(3), 1015-1032, 2018

IV Emadeldeen Hassan, Eddie Wadbro, Linus Hägg, and Martin Berggren, *Topology optimization of compact wideband coaxial-to-waveguide transitions with minimum-size control.* Structural and Multidisciplinary Optimization, 57(4), 1765-1777, 2018

Part II is based on the following publications

V Martin Berggren and Linus Hägg, *Well-posed variational formulations of Friedrichs-type systems.* 2020, arXiv:2004.12778

VI Linus Hägg and Martin Berggren, *On the well-posedness of Galbrun's equation.* 2020, arXiv:1912.04364

[3] http://creativecommons.org/licenses/by/4.0/

Author contributions

Publications I – III were developed and authored in close cooperation between Hägg and Wadbro.

Publication I. Hägg was the main responsible for conceiving the fW-mean filter framework, while Wadbro was the main responsible for the presented summation algorithm and numerical experiments.

Publication II. Hägg had the main responsibility for the theoretical development, except for the proof of Theorem 1, which truly was a team effort. Wadbro was the main responsible for the numerical experiments presented in the article, although, Hägg performed some preliminary numerical studies on the optimization of cantilever beams, and provided the source code excerpts presented in the article.

Publication III. Hägg was the main responsible for the theoretical development, while Wadbro had the main responsibility for the numerical experiments. In particular, Hägg was responsible for the characterization of minimum length scale expressed by Theorem 3, and the idea to assess the minimum length scales of the optimized designs quantitatively.

Publication IV. Hägg mainly contributed to devising and implementing the filter schemes, and authored parts of the manuscript.

Publication V. Hägg mainly contributed to the third example. In particular, Hägg was the main responsible for Theorem 5.9 and the proof of Lemma 5.5. Hägg also contributed with comments and suggestions to the other two examples.

Publication VI. With invaluable guidance by Berggren, Hägg was responsible for developing Publication VI.

Contents

Notations and conventions

Measure symbols are omitted from integrals whenever the type of measure (volume, surface, or line measure) is evident from the domain of integration.

$\bar{\mathbb{R}} = \mathbb{R} \cup \{-\infty, \infty\}$ denotes the extended real numbers.

Let $M \subset \mathbb{R}^d$.
$M^{\complement} = \mathbb{R}^d \setminus M$ denotes the complement of M.
$rM = \{x \in \mathbb{R}^d \mid r^{-1}x \in M\}$ denotes the scaling of M by $r \neq 0$.
$x + M = \{x \in \mathbb{R}^d \mid m - x \in M\}$ denotes the translation of M by $x \in \mathbb{R}^d$.
χ_M denotes the indicator function of M, that is,

$$\chi_M(x) = \begin{cases} 1 & x \in M, \\ 0 & x \notin M. \end{cases}$$

If M is Lebesgue measurable, then $|M| = \int_{\mathbb{R}^d} \chi_M$ denotes the Lebesgue measure of M.

For $f : [0,1] \to \mathbb{R}$ and $\boldsymbol{\rho} = (\rho_1, \rho_2, \ldots, \rho_n)^T \in [0,1]^n \subset \mathbb{R}^n$, we define $\boldsymbol{f} : [0,1]^n \to \mathbb{R}^n$ by $\boldsymbol{f}(\boldsymbol{\rho}) = (f(\rho_1), f(\rho_2), \ldots, f(\rho_n))^T$.

$\mathbf{1}_{\boldsymbol{n}} = (1, 1, \ldots, 1)^T \in \mathbb{R}^n$.

Part I
The fW-mean Filter Framework for Topology Optimization

1. Computational design optimization

Successful hardware designs strike a balance between functionality and aesthetics, adhere to hardware specifications, and are producible at reasonable costs. In case there are many possible designs that satisfy the hardware specifications, it is natural to strive for one that is optimal in some desirable sense. This thesis focuses on design problems where the desired performance is measured by an objective function, which may depend explicitly or implicitly on some design defining parameters. In particular, we consider so-called *computational design optimization problems* for which the performance of the considered device can be accurately predicted and optimized by numerically evaluating and extremizing the objective function with respect to the design parameters.

The strategy of most optimization algorithms is to improve the performance gradually by iteratively updating the design. In fact, design optimization methods are often classified by the complexity of their update. *Sizing optimization* is the simplest form of design optimization in which the sizes of the constituent parts of a given configuration are optimized. A design optimization method that does not only optimize the *sizes* of the constituent parts of a given device but also their *shapes* is classified as *boundary shape optimization*. In this thesis, we consider *topology optimization*, which by far is the most general form of design optimization, in which the *size*, *shape*, and *connectedness* of the device are subject to optimization.

2. Density based topology optimization

The aim of topology optimization algorithms is to find a layout of material that maximizes a given performance measure. Over the years, different topology optimization approaches that result from different ways of representing the layout of material have been proposed [23, 54].

In this thesis, we consider *density based topology optimization* in which the layout of a single material in a given design domain $\Omega \subset \mathbb{R}^d$ is represented by the material indicator function

$$\rho : \Omega \to \{0, 1\}, \tag{2.1}$$

as illustrated in Figure 5. Density based topology optimization of linearly elastic

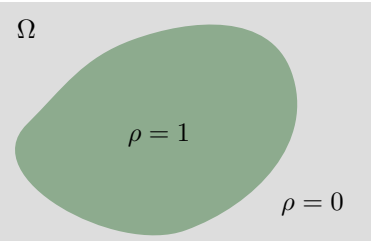

Figure 5: In density based topology optimization the layout of material is represented by the indicator function $\rho : \Omega \to \{0, 1\}$.

structures has its roots in the work of Bendsøe & Kikuchi [3], and a comprehensive account of the subject is given in the monograph by Bendsøe & Sigmund [4]. The standard approach used to discretize topology optimization problems is to partition the design domain Ω into $n \in \mathbb{N}$ elements using a Cartesian grid and introduce a *design vector* $\boldsymbol{\rho} \in \{0, 1\}^n$ that indicates the presence or absence of material at each element. For 2D design domains, it is customary to visualize the design vector as a binary image by interpreting each element i as a pixel, which is either black or white depending on the value of ρ_i. The approximate solution to the design problem satisfies the integer optimization problem

$$\min_{\boldsymbol{\rho} \in \{0,1\}^n} J(\boldsymbol{\rho}) \text{ subject to } \boldsymbol{C}(\boldsymbol{\rho}) \leq \mathbf{0}, \tag{2.2}$$

where $J : \{0, 1\}^n \to \mathbb{R}$ is the (discretized) objective function[1] and $\boldsymbol{C} : \{0, 1\}^n \to \mathbb{R}^m$ encodes $m \geq 0$ constraints on the design vector. In the applications considered in this thesis, the objective function is evaluated by computer simulations. Unfortunately, problem (2.2) is computationally intractable for most realistic design problems as the number of design variables $n \gg 1$, even more so if the design problem

[1] It is standard practice to employ a minimization formulation of the design problem, but note that a maximization formulation could be obtained by changing J to $-J$.

should be solved to *global* optimality. If the (discretized) objective and constraint functions extend to differentiable functions on $[0,1]^n$, problem (2.2) may be relaxed by allowing design vectors with intermediate values $\boldsymbol{\rho} \in [0,1]^n$,

$$\min_{\boldsymbol{\rho}\in[0,1]^n} J(\boldsymbol{\rho}) \text{ subject to } \boldsymbol{C}(\boldsymbol{\rho}) \leq \mathbf{0}, \tag{2.3}$$

where J and $\boldsymbol{C}$ now refer to the extended objective and constraint functions. In this context, it is common to refer to the relaxed design vector as the density. The relaxed optimization problem (2.3) has the advantage that it often can be (approximately) solved by employing gradient based optimization algorithms, which can be constructed to efficiently handle many design variables. However, in most circumstances, the relaxation comes at a cost. Namely, at convergence of the optimization algorithm, the design vector is likely to be non-binary and only *locally* optimal. There are techniques intended to prevent the optimization algorithm from converging to badly performing local optima. In general, non-binary designs are difficult to interpret and may even be unphysical. Nevertheless, in some cases, intermediate values can be shown to represent the effective behavior of materials with microstructures. This thesis, however, considers only methods that attempt to minimize the amount of intermediate values $\rho_i \in (0,1)$ by implicit or explicit penalization. Unfortunately, the (approximate) solutions to the penalized–relaxed optimization problem typically depend strongly on the particular partition of the design domain and fail to converge when the partition is refined. It is important to note that such mesh-dependence is also present in the original binary topology optimization problem (2.2). A number of different strategies have been devised to counter the issue of mesh-dependence [14]. The most popular strategy has been to introduce a regularizing (density) filter operator

$$\boldsymbol{F} : [0,1]^n \to [0,1]^n \tag{2.4}$$

and replace the extended objective and constraint functions with $J \circ \boldsymbol{F}$ and $\boldsymbol{C} \circ \boldsymbol{F}$, respectively. We note that the effect of replacing the extended objective and constraint functions is similar to that of restricting the design vectors to be in the image $\boldsymbol{F}([0,1]^n)$. In general, the quantity $\boldsymbol{F}(\boldsymbol{\rho})$ is preferably used as the manufacturing blueprint and is therefore often referred to as the *physical design* in the literature.

3. The minimum compliance problem

The prototype problem in density based topology optimization is to determine the layout of a linearly elastic structure of given volume, which is subject to static supports and loads, so that the compliance is minimized. Although the precise definition of compliance will be given later, we note that compliance is an inverse measure of stiffness, so minimizing the compliance is a way of maximizing the stiffness of the structure.

Elastic materials deform under loads but resume their unloaded form when the load is removed. Many solid construction materials are linearly elastic for small deformations, that is, load-induced deformations depend linearly on the applied load. The linear relationship between deformation and stress is expressed in Hooke's law

$$\sigma = E\epsilon, \tag{3.1}$$

where σ denotes the symmetric second order stress tensor, E the fourth order elasticity tensor, and ϵ the symmetric second order (infinitesimal) strain tensor. The elasticity tensor obeys the symmetries [32, § 29]

$$E_{ijkl} = E_{jikl} = E_{ijlk} = E_{klij}. \tag{3.2}$$

Given the stress tensor, the force that acts on any part $\hat{\Omega}$ of a linear elastic body in static equilibrium is given by

$$\hat{f} = -\int_{\partial\hat{\Omega}} \sigma n, \tag{3.3}$$

where n denotes the outward unit normal to the boundary $\partial\hat{\Omega}$. The infinitesimal strain tensor measures the local deformation and is given by the formula

$$\epsilon = \frac{1}{2}(\nabla u + \nabla u^T), \tag{3.4}$$

where u denotes the displacement vector field, which is such that $x + u(x)$ gives the location in the deformed body of material located at x in the undeformed body.

The equilibrium displacement field u of a finite linearly elastic body $\Omega \subset \mathbb{R}^d$ that is clamped along the boundary part Γ_D satisfies the variational equation

$$a(u, v) := \int_\Omega \epsilon(v) : \underbrace{E\epsilon(u)}_{=\sigma(u)} = \int_\Omega v \cdot b \;+ \int_{\partial\Omega\setminus\Gamma_D} v \cdot t =: l(v), \tag{3.5}$$

where v is any sufficiently regular vector field that vanishes on Γ_D, $\epsilon(v) : \sigma(u) = \sigma(u) : \epsilon(v) = \sum_{ij} \sigma_{ij}(u)\epsilon_{ij}(v)$, and b and t are the volume and surface force densities of the forces acting on the body, respectively. Equation (3.5) is a variational form of the static equilibrium equations, expressing balance of forces for any sub-body, suitable for mathematical analysis and computation. In fact, equation (3.5) will be the basis for defining the equilibrium displacement field. To that end, we assume that

the region occupied by the (unloaded) body $\Omega \subset \mathbb{R}^d$ is open, bounded, connected, and lies locally on one side of its Lipschitz continuous boundary $\partial\Omega$, $\Gamma_D \subset \partial\Omega$ is nonempty and open, and we introduce the Hilbert space of kinematically admissible displacement fields

$$\mathcal{U} = \{u \in H^1(\Omega)^d \mid u = 0 \text{ on } \Gamma_D\}, \tag{3.6}$$

equipped with the norm $\|\cdot\|_{\mathcal{U}} \coloneqq \|\cdot\|_{H^1(\Omega)^d}$. To make the integrals in equation (3.5) well-defined for $u, v \in \mathcal{U}$, we assume that E is essentially bounded, $b \in L^2(\Omega)^d$, and $t \in L^2(\partial\Omega \setminus \bar{\Gamma}_D)^d$. Moreover, we assume that E is positive definite in the sense that there exists a constant $C_1 > 0$ such that, for any symmetric constant second order tensor S,

$$S : ES \geq C_1 S : S \text{ almost everywhere in } \Omega. \tag{3.7}$$

Since E is essentially bounded and positive definite (3.7), it follows from Korn's inequality [22, Thm. 6.15-4] that the bilinear form $a : \mathcal{U} \times \mathcal{U} \to \mathbb{R}$ in expression (3.5) is bounded and coercive. That is, there are constants C_2 and $C_3 > 0$ such that, for any $u, v \in \mathcal{U}$,

$$|a(u, v)| \leq C_2 \|u\|_{\mathcal{U}} \|v\|_{\mathcal{U}}, \tag{3.8}$$

$$a(u, u) \geq C_3 \|u\|_{\mathcal{U}}^2. \tag{3.9}$$

Moreover, the assumptions on b and t imply that the (load) linear form $l : \mathcal{U} \to \mathbb{R}$ is bounded; that is, there is some constant C_4 such that, for any $u \in \mathcal{U}$,

$$|l(u)| \leq C_4 \|u\|_{\mathcal{U}}. \tag{3.10}$$

Employing the Lax–Milgram lemma [22, Thm. 6.2-1], we conclude that the equilibrium displacement u is well-defined as the solution to the following variational problem.

$$\text{Find } u \in \mathcal{U} \text{ such that equation (3.5) holds for all } v \in \mathcal{U}. \tag{3.11}$$

The *compliance* of a linearly elastic structure is defined as the total work performed by the applied forces, $l(u)$, where l is the linear form defined by the expression in equation (3.5) and u the unique equilibrium displacement field defined as the solution to the variational problem (3.11). By the definition of u (3.11), we find

$$l(u) = a(u, u). \tag{3.12}$$

That is, at equilibrium, the work $l(u)$ of the applied forces is proportional the stored elastic energy $\frac{1}{2}a(u, u)$. Thus, minimization of the compliance is equivalent to minimizing the stored elastic energy.

Here, we consider topology optimization of the layout of a fixed homogeneous and isotropic linearly elastic material characterized by the elasticity tensor E_1. We introduce the set of relaxed indicator functions

$$\mathcal{D} \coloneqq \{\rho \in L^\infty(\Omega) \mid 0 \leq \rho \leq 1 \text{ almost everywhere in } \Omega\}, \tag{3.13}$$

and note that the layout of the fixed material within Ω can be represented by some $\rho \in \mathcal{D}$ such that $\rho \in \{0, 1\}$ almost everywhere in Ω. To be precise, regions that are

occupied with the fixed material correspond to the value $\rho = 1$, while void regions correspond to $\rho = 0$. To facilitate the mathematical analysis and computation of (approximate) solutions to the minimum compliance problem, we approximate void with a very compliant material with elasticity tensor $\underline{\rho} E_1$ for some $0 < \underline{\rho} \ll 1$. The effect of different designs $\rho \in \mathcal{D}$ on the compliance is captured by introducing the parametrized elasticity tensor

$$E(\rho) = \left(\underline{\rho} + \left(1 - \underline{\rho}\right) P(\rho)\right) E_1 \tag{3.14}$$

in equation (3.5). The rationale behind the penalty operator $P : \mathcal{D} \to \mathcal{D}$ introduced in expression (3.14) will be described later, and for now we may ignore its effect by letting P to be the identity operator on $\mathcal{D}$. Note that $E(\rho)$ is essentially bounded and satisfies the positivity condition (3.7) for any $\rho \in \mathcal{D}$, since $\underline{\rho} > 0$. Thus, variational problem (3.11) is uniquely solvable and associates a unique displacement field $u \in \mathcal{U}$ to any $\rho \in \mathcal{D}$. Let G denote the corresponding mapping from $\mathcal{D}$ to $\mathcal{U}$.

The set of feasible designs $\mathcal{A}$ contains those elements in $\mathcal{D}$ that also satisfy additional constraints, that is,

$$\mathcal{A} = \{\rho \in \mathcal{D} \mid C_i(\rho) \leq 0 \, \forall i \in \mathcal{I}\}, \tag{3.15}$$

where $\mathcal{I}$ numbers the constraint functionals $C_i : \mathcal{D} \to \mathbb{R}$. Here, we consider the so-called volume[1] constraint

$$C_1(\rho) \coloneqq \int_\Omega \rho - V \leq 0, \tag{3.16}$$

which imposes an upper bound $V > 0$ on the amount of material within Ω. Since the compliance (3.12) decreases if material is added to a design, it is expected that a solution ρ to the minimum compliance problem attains the volume bound V, that is, $C_1(\rho) = 0$. The amount of intermediate values $\rho \in (0, 1)$ can be controlled by introducing the constraint

$$C_2(\rho) \coloneqq \int_\Omega \rho(1 - \rho) - c_2 \leq 0, \tag{3.17}$$

where $c_2 \geq 0$. Note that $C_2(\rho) \geq -c_2$ for any $\rho \in \mathcal{D}$. Thus, if $c_2 = 0$, constraint (3.17) forces $\rho \in \{0, 1\}$ almost everywhere in Ω. In the presence of the volume constraint (3.16), the amount of intermediate values may also be controlled by invoking a penalty operator P in expression (3.14) that makes the contribution to the stiffness of intermediate densities $\rho \in (0, 1)$ disproportionately small compared to their contribution to the volume constraint (3.16). For instance, this effect may be achieved by defining $P : \mathcal{D} \to \mathcal{D}$ by $P(\rho) = f_p \circ \rho$, where $f_p : \bar{\mathbb{R}} \to \bar{\mathbb{R}}$ depends on a real parameter p and whose restriction $f_p|_{[0,1]} : [0, 1] \to [0, 1]$ is smooth, strictly increasing, and satisfies $f_p(0) = 0, f_p(1) = 1$, and $f_p(s) < s$ for all $s \in (0, 1)$. The SIMP scheme (Solid Isotropic Material with Penalization), which is extensively used in the literature, results from

$$f_p|_{[0,1]}(s) = s^p \tag{3.18}$$

[1] If $\rho \in \{0, 1\}$ almost everywhere in Ω, $\int_\Omega \rho$ gives the volume of the fixed material.

for some $p > 1$.

By introducing the objective functional $J \coloneqq l \circ G : \mathcal{D} \to \mathbb{R}$, where, as before, $G : \mathcal{D} \to \mathcal{U}$ maps any $\rho \in \mathcal{D}$ to the corresponding equilibrium displacement $u \in \mathcal{U}$, we may formulate the minimum compliance problem as follows.

$$\text{Find } \rho^* \in \mathcal{A} \text{ such that } J(\rho^*) \leq J(\rho) \text{ for any } \rho \in \mathcal{A}. \tag{3.19}$$

The following is an alternative formulation of the minimum compliance problem.

$$\text{Find } u^* \in G(\mathcal{A}) \text{ such that } l(u^*) \leq l(u) \text{ for any } u \in G(\mathcal{A}). \tag{3.20}$$

Note that solutions to problem (3.19) exist if and only if solutions to problem (3.20) exist.

If intermediate values are not penalized, then there are solutions to the minimum compliance problem and the optimal equilibrium displacement is unique [4, § 5.2.1]. In 2D, this problem is known as the variable thickness sheet problem, since $E(\rho) = \left(\underline{\rho} + \left(1 - \underline{\rho}\right) \rho\right) E_1$ may be interpreted as the elasticity tensor corresponding to a sheet with variable thickness $\underline{\rho} + \left(1 - \underline{\rho}\right) \rho$. However, if intermediate values are penalized (either by imposing constraint (3.17) or by using a suitable penalty operator P), there are no solutions to the minimum compliance problem.

To resolve the ill-posedness of the penalized minimum compliance problem, we may restrict the set of feasible designs [13]. Typically, the cost of restricting the set of feasible designs is a degraded performance of the optimal solutions. In a broad sense, restricting the problem by bounding the gradient of ρ is known to resolve the ill-posedness [14]. A noteworthy example of that general technique is to restrict the problem by imposing an upper bound on the total variation of the design field, which bounds the perimeter of the design [48]. An alternative to directly bounding the gradient of ρ is to restrict the design field to the image of a suitable filter operator $F : \mathcal{D} \to \mathcal{D}$ by replacing the objective and constraint functionals with $J \circ F$ and $C_i \circ F$. Bourdin [16] demonstrated that applying a *linear* filter operator, defined as the convolution with a positive, normalized, and compactly supported kernel, resolves the ill-posedness of the SIMP-penalized minimum compliance problem. The main theoretical result of Publication II is Theorem 1, which is an extension of Bourdin's result to (sequences of) *nonlinear* filters of the form

$$F(\rho) \coloneqq g \circ W(f \circ \rho), \tag{3.21}$$

where $f, g : [0,1] \to [0,1]$ are continuous[2] and surjective, $W : \mathcal{D} \to \mathcal{D}$ is a *linear* integral operator defined by

$$W(\rho)(x) = \int_\Omega w(x,y)\rho(y)\,\mathrm{d}y, \tag{3.22}$$

where the kernel $w : \Omega \times \Omega \to \bar{\mathbb{R}}$ is measurable, non-negative, and normalized,

$$w \geq 0 \text{ almost everywhere in } \Omega \times \Omega, \tag{3.23}$$

$$\int_\Omega w(x,y)\,\mathrm{d}y = 1 \text{ for almost all } x \in \Omega. \tag{3.24}$$

[2] In practice, f and g are required to be more regular.

We call filters of the form (3.21) *generalized fW-mean filters*. If $g = f^{-1}$, we call the resulting subclass of filters *fW-mean filters*, since these are based on infinite dimensional versions of weighted quasi-arithmetic averages, also known as f-means. Borvall & Petersson [15] suggest yet another strategy that guarantees the existence of solutions to the penalized minimum compliance problem. Their strategy is to replace the constraint functional C_2 in the constraint (3.17) by $C_2 \circ W$, where W is a linear (filter) operator of the form (3.22), constructed so that $C_2(\rho) \leq C_2(W\rho)$, which guarantees proper penalization of intermediate values of the design field.

The standard approach used to discretize the minimum compliance problem is to make a Cartesian partition of the design domain into $n \in \mathbb{N}$ equally sized elements[3], and to restrict the relaxed indicator function ρ to be piecewise constant on the elements. The piecewise constant ρ may be represented by the design vector $\boldsymbol{\rho} \in [0,1]^n$ containing the values of the piecewise constant design field at each of the elements. Here, we only consider penalization of intermediate values by a penalty operator P defined via a suitable function f_p, such as the function (3.18) that defines the SIMP scheme. The preferred choice for discretizing the variational equation (3.5) is the finite element method. A conformal finite element approximation with $N + M$ nodes leads to the linear system

$$\boldsymbol{K}(\boldsymbol{\rho})\boldsymbol{u} = \boldsymbol{b}, \tag{3.25}$$

where $\boldsymbol{K}(\boldsymbol{\rho}) \in \mathbb{R}^{dN \times dN}$ is called the stiffness matrix, $\boldsymbol{u} \in \mathbb{R}^{dN}$ the vector of nodal displacements, and $\boldsymbol{b} \in \mathbb{R}^{dN}$ the nodal load vector. The remaining M nodes are left out of equation (3.25) since they are located on Γ_D, where the nodal displacements are known to vanish due to the clamping of the structure. The stiffness matrix can be expressed as a sum of element contributions,

$$\boldsymbol{K}(\boldsymbol{\rho}) = \sum_{i=1}^{n} \left(\underline{\rho} + \left(1 - \underline{\rho}\right) f_p(\rho_i)\right) \boldsymbol{K}_i, \tag{3.26}$$

where $\boldsymbol{K}_i$ gives the element stiffness matrix of element i in the case that this element is occupied with the fixed material. The symmetries (3.2) of the elasticity tensor, and the coerciveness (3.9) of the bilinear form a in equation (3.5) imply that the stiffness matrix is symmetric and positive definite.

The discrete analogue of the volume constraint (3.16) is given by

$$C_1(\boldsymbol{\rho}) \coloneqq \sum_{i=1}^{n} h^d \rho_i - V = h^d \mathbf{1}_{\boldsymbol{n}}^T \boldsymbol{\rho} - V \leq 0, \tag{3.27}$$

where h^d denotes the measure (volume or area) of an element in the Cartesian partition. Letting

$$j(\boldsymbol{u}) \coloneqq \boldsymbol{b}^T \boldsymbol{u} \tag{3.28}$$

be the discrete analogue of the compliance (3.12) and defining

$$J(\boldsymbol{\rho}) \coloneqq \boldsymbol{b}^T \boldsymbol{K}(\boldsymbol{\rho})^{-1} \boldsymbol{b} \, (= \boldsymbol{b}^T \boldsymbol{u} = j(\boldsymbol{u})), \tag{3.29}$$

[3] Other types of partitions are possible. However, the Cartesian partition with equally sized elements is often preferred as it imposes little prior bias on the designs and leads to simple and efficient computer implementations.

we may formulate the discretized penalized minimum compliance problem as

$$\min_{\boldsymbol{\rho}\in[0,1]^n} J(\boldsymbol{\rho}) = \boldsymbol{b}^T \boldsymbol{K}(\boldsymbol{\rho})^{-1}\boldsymbol{b} \text{ such that } C_1(\boldsymbol{\rho}) = h^d \mathbf{1}_{\boldsymbol{n}}^T \boldsymbol{\rho} - V \leq 0. \tag{3.30}$$

We note that it is not necessary, nor advisable from a computational point of view, to compute $\boldsymbol{K}(\boldsymbol{\rho})^{-1}$, as it suffices to compute $\boldsymbol{u} = \boldsymbol{K}(\boldsymbol{\rho})^{-1}\boldsymbol{b}$ by solving the linear system (3.25).

To generate (approximate) solutions to problem (3.30) by gradient based optimization algorithms, derivatives of the objective and constraint functions with respect to the design variables need to be computed. The derivatives of the constraint function are found by differentiating the defining expression (3.27),

$$\frac{\partial C_1}{\partial \rho_i} = h^d. \tag{3.31}$$

In general, the adjoint sensitivity method [21, § 6.2.2] is the preferred method for determining the gradient of an objective or constraint function that depends on $\boldsymbol{\rho}$ via $\boldsymbol{u}$, such as the compliance (3.29). Nevertheless, due to the very special structure of the current problem, the gradient of the objective function (3.29) may be determined by a more direct two-step procedure. First, using that $J(\boldsymbol{\rho}) = j(\boldsymbol{u}) = \boldsymbol{b}^T\boldsymbol{u}$, where $\boldsymbol{u} = \boldsymbol{K}(\boldsymbol{\rho})^{-1}\boldsymbol{b}$, and that $\boldsymbol{b}$ is independent of $\boldsymbol{\rho}$, we find

$$\frac{\partial J}{\partial \rho_i} = \boldsymbol{b}^T \frac{\partial \boldsymbol{u}}{\partial \rho_i} = \boldsymbol{u}^T \boldsymbol{K} \frac{\partial \boldsymbol{u}}{\partial \rho_i}, \tag{3.32}$$

where the substitution $\boldsymbol{b}^T = \boldsymbol{u}^T\boldsymbol{K}$ follows from equation (3.25) and the symmetry of the stiffness matrix. Second, differentiating equation (3.25), we find

$$\frac{\partial \boldsymbol{K}}{\partial \rho_i}\boldsymbol{u} + \boldsymbol{K}\frac{\partial \boldsymbol{u}}{\partial \rho_i} = \frac{\partial \boldsymbol{b}}{\partial \rho_i} = 0. \tag{3.33}$$

Thus, combining expressions (3.32) and (3.33), we obtain

$$\frac{\partial J}{\partial \rho_i} = -\boldsymbol{u}^T \frac{\partial \boldsymbol{K}}{\partial \rho_i}\boldsymbol{u}. \tag{3.34}$$

Differentiating expression (3.26), we find

$$\frac{\partial \boldsymbol{K}}{\partial \rho_i} = (1-\underline{\rho}) f_p'(\rho_i)\boldsymbol{K}_i, \tag{3.35}$$

which is positive semi-definite by construction. Thus, combining expressions (3.34) and (3.35), we reveal that

$$\frac{\partial J}{\partial \rho_i} \leq 0. \tag{3.36}$$

Thus, we cannot increase the compliance by increasing ρ_i. This peculiarity is exploited in the so-called optimality criteria method [4, § 1.2.1], which is routinely applied to compute (approximate) solutions to the compliance minimization problem (3.30). However, property (3.36) cannot be expected to hold for other density based topology optimization problems, which require general-purpose gradient-based optimization algorithms such as the method of moving asymptotes [57, 58].

Although there are no solutions to the infinite dimensional penalized minimum compliance problem (3.19), there are always solutions to the discretized penalized minimum compliance problem (3.30). However, the solutions may depend strongly on the partition of the design domain and represent designs with details that get smaller and smaller when the partition is refined. As already mentioned, a number of different approaches have been proposed to resolve this mesh-dependency issue. In this thesis, we consider replacing the objective and constraint functions (3.29) and (3.27) with $J \circ \boldsymbol{F}$ and $C_1 \circ \boldsymbol{F}$, where $\boldsymbol{F} : [0,1]^n \to [0,1]^n$ is a filter operator to be specified later. For now, we only note that the filter operators to be considered are smooth and satisfy

$$\frac{\partial F_j}{\partial \rho_i} \geq 0. \tag{3.37}$$

Applying the chain rule and expression (3.31), we find

$$\frac{\partial}{\partial \rho_i} C_1 \circ \boldsymbol{F} = \sum_{j=1}^{n} h^d \frac{\partial F_j}{\partial \rho_i} = h^d \mathbf{1}_{\boldsymbol{n}}^T \frac{\partial \boldsymbol{F}}{\partial \rho_i}. \tag{3.38}$$

Similarly, the chain rule and expression (3.34) yields

$$\frac{\partial}{\partial \rho_i} J \circ \boldsymbol{F} = -\boldsymbol{u}^T \left(\frac{\partial}{\partial \rho_i} \boldsymbol{K} \circ \boldsymbol{F} \right) \boldsymbol{u}, \tag{3.39}$$

where $\boldsymbol{u}$ is the unique solution to $(\boldsymbol{K} \circ \boldsymbol{F})\boldsymbol{u} = \boldsymbol{b}$. Moreover, the chain rule and expression (3.35) yields

$$\frac{\partial}{\partial \rho_i} \boldsymbol{K} \circ \boldsymbol{F} = \sum_{j=1}^{n} \left(1 - \underline{\rho}\right) f_p' \circ F_j \boldsymbol{K}_j \frac{\partial F_j}{\partial \rho_i}, \tag{3.40}$$

which is positive semi-definite by bound (3.37). Thus, combining expressions (3.39) and (3.40), we reveal that

$$\frac{\partial}{\partial \rho_i} J \circ \boldsymbol{F} \leq 0. \tag{3.41}$$

Thus, the property that we cannot increase the compliance by increasing ρ_i is preserved by the filter.

Bendsøe & Sigmund [4, § 1.3.3] remark that complementing gradient based optimization algorithms with *continuation approaches* often lead to improved results. The idea of a continuation approach is to solve (or approximately solve) a sequence of optimization problems that approach (either approximately or exactly) the desired, not so well-behaved, optimization problem, starting with some simple and well-behaved optimization problem and initializing subsequent optimization problems with the solution of the previous problem. Hopefully, such strategy prevents the gradient-based optimizer from converging to badly performing local optima. For the minimum compliance problem, we may solve a sequence of optimization problems corresponding to an increasing sequence of the penalty parameter p in formula (3.18), starting with $p = 1$, which corresponds to (an approximation of) the variable thickness sheet problem. In this thesis, we employ continuation over the penalty parameter p in formula (3.18), as well as over the filter parameters such as α (β) introduced in Section 5.2. It should be noted that continuation is not always successful [55].

3.1 The minimum "heat compliance" problem

In the so-called minimum "heat compliance" problem, we want to find a layout in $\Omega \subset \mathbb{R}^d$ of a heat conducting material that minimizes the average static equilibrium temperature

$$l(u) \coloneqq \frac{1}{|\Omega|} \int_\Omega u, \tag{3.42}$$

when there is a uniform source of heat within Ω, and $\partial\Omega$ is thermally insulated, except at the part Γ_D, which is held at zero temperature. In this case, the static equilibrium temperature u satisfies the variational equation

$$a(u, v) \coloneqq \int_\Omega \kappa \nabla v \cdot \nabla u = l(v), \tag{3.43}$$

where v is any sufficiently regular scalar field that vanishes on Γ_D, and κ is the spatially variable heat conductivity. We assume that Ω is open, bounded, connected, and lies locally on one side of its Lipschitz continuous boundary $\partial\Omega$. Moreover, we assume that $\Gamma_D \subset \partial\Omega$ is nonempty and open, and that $0 < \underline{\kappa} \leq \kappa \leq \overline{\kappa} < \infty$ almost everywhere in Ω. Defining the Hilbert space $\mathcal{U} = \{u \in H^1(\Omega) \mid u = 0 \text{ on } \Gamma_D\}$ equipped with the norm $\|\cdot\|_{\mathcal{U}} = \|\cdot\|_{H^1(\Omega)}$, we find that the bilinear form $a : \mathcal{U} \times \mathcal{U} \to \mathbb{R}$ and linear form $l : \mathcal{U} \to \mathbb{R}$ in equation (3.43) are bounded. Moreover, by the Poincaré inequality [22, Thm. 6.5-2] and the positivity of κ, the bilinear form a is coercive. Thus, by the Lax–Milgram lemma [22, Thm. 6.2-1], the static equilibrium temperature is the unique solution to the following variational problem.

$$\text{Find } u \in \mathcal{U} \text{ such that equation (3.43) holds for all } v \in \mathcal{U}. \tag{3.44}$$

Here we consider the layout of a fixed homogeneous (and isotropic) material with thermal conductivity $\kappa_1 > 0$. Introducing the parametrized thermal conductivity

$$\kappa(\rho) = \big(\underline{\rho} + \big(1 - \underline{\rho}\big)\, P(\rho)\big)\, \kappa_1, \tag{3.45}$$

we may proceed analogously as for the minimum compliance problem. However, since temperature is a *scalar* field, the computational burden of the finite element approximation is significantly less than that for the displacement *vector* field in elasticity. We note that, for any $0 < \underline{\rho} < 1$, the minimum "heat compliance" problem concerns the optimal layout of *two* materials, one with "high" thermal conductivity κ_1 and one with "low" thermal conductivity $\kappa_0 \coloneqq \underline{\rho}\kappa_1 < \kappa_1$.

4. Imposing minimum size

The rationale behind imposing minimum sizes on some of the material phases in design optimization is two-fold. From a manufacturing point of view, fine details are expected to be difficult and expensive to manufacture. The other reason to impose minimum sizes is of a more mathematical and computational nature. As described in the previous section, unless some action is taken, the numerical solutions of the discretized penalized minimum compliance problems may exhibit ever finer details as the discretization is refined.

An intuitive and widespread characterization [16, 18, 30, 31, 53, 59] of a length scale states that *a region $M \subset \mathbb{R}^d$ has a minimum length scale greater than or equal to $r > 0$ if any point $x \in M$ belongs to some d-dimensional ball of radius r that is completely contained in M.* In Publication III, we formalize the intuitive characterization by defining the *local length scale* of an open set M at $x \in M$ as the radius of the largest ball that contains x and is completely contained in M, and the *minimum length scale* of M as the smallest local length scale, that is,

$$R_B(M) \coloneqq \inf_{x \in M} \sup\{r > 0 \mid \exists m \in M \text{ s.t. } x \in m + rB \subset M\}, \tag{4.1}$$

where $rB \subset \mathbb{R}^d$ is the scaled open unit ball[1] $B \subset \mathbb{R}^d$. Other notions of minimum length scale are briefly reviewed in Publication III.

The intuitive characterization of length scale is tightly connected to the *dilation* operation

$$\mathcal{D}_{rB}(M) \coloneqq \bigcup_{x \in M} (x + rB). \tag{4.2}$$

It is evident from definition (4.2) that, for any nonempty $M \subset \mathbb{R}^d$, the minimum length scale of $\mathcal{D}_{rB}(M)$ is at least r. The complementary operation of dilation is called *erosion*,

$$\mathcal{E}_{rB}(M) \coloneqq \bigcap_{x \in M} (x + rB), \tag{4.3}$$

$$\mathcal{E}_{rB}(M)^{\complement} = \mathcal{D}_{rB}\left(M^{\complement}\right). \tag{4.4}$$

Dilation and erosion are two of the basic operations defined in mathematical morphology, which is a branch of image analysis. Here, we provide only a condensed presentation of mathematical morphology, and refer to Publication III, or the comprehensive review by Heijmans [36] for details. In the context of mathematical morphology, rB is called the structuring element. The (morphological) *open* and *close* operators are defined by composing the (morphological) dilate and erode operators, that is,

$$\mathcal{O}_{rB} \coloneqq \mathcal{D}_{rB} \circ \mathcal{E}_{rB}, \tag{4.5}$$

$$\mathcal{C}_{rB} \coloneqq \mathcal{E}_{rB} \circ \mathcal{D}_{rB}, \tag{4.6}$$

[1] Not necessarily the Euclidean unit ball.

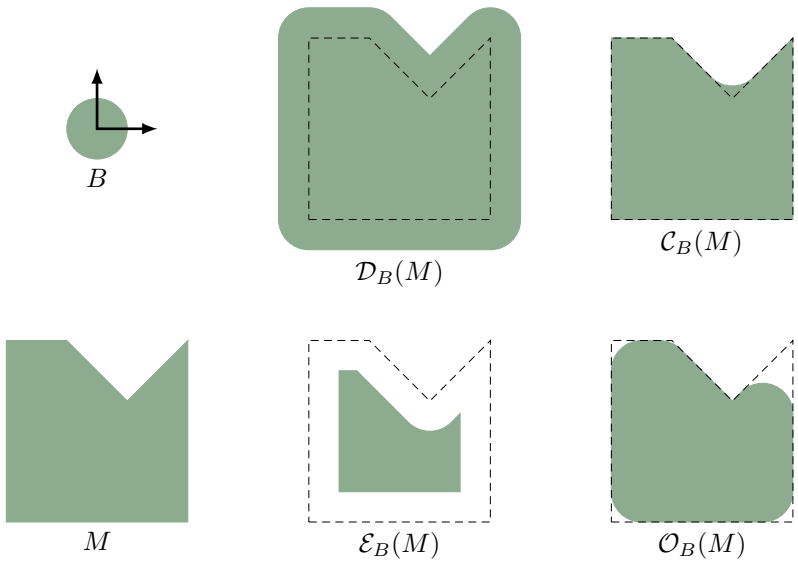

Figure 6: Illustration of morphological operators.

respectively. The open and close operators are idempotent and satisfy the ordering

$$\mathcal{O}_{rB}(\mathcal{O}_{rB}(M)) = \mathcal{O}_{rB}(M) \subset M \subset \mathcal{C}_{rB}(M) = \mathcal{C}_{rB}(\mathcal{C}_{rB}(M)) \tag{4.7}$$

for any $M \subset \mathbb{R}^d$. Figure 6, which originates from Publication III, exemplifies the different morphological operations.

A rigorous connection between the minimum length scale (4.1) and mathematical morphology is established as a special case of Theorem 3 in Publication III, which informally says that the minimum length scale $R_B(M)$, of a nonempty region $M \subset \mathbb{R}^d$, is the largest r such that $M = \mathcal{O}_{rB}(M)$.

For functions $\rho : \mathbb{R}^d \to [0,1]$ the dilation and the erosion are functions $: \mathbb{R}^d \to [0,1]$ defined by the expressions

$$\mathcal{D}_{rB}(\rho)(x) \coloneqq \sup_{y \in x + rB} \rho(y), \tag{4.8}$$

$$\mathcal{E}_{rB}(\rho)(x) \coloneqq \inf_{y \in x + rB} \rho(y), \tag{4.9}$$

respectively. Beware that the same symbol is used to denote morphological operations on functions and on sets; in any instance, the argument of the operator determines which definition is implied. Definitions (4.8) and (4.9) for functions are consistent with definitions (4.2) and (4.3) for sets in the sense that, for any $M \subset \mathbb{R}^d$,

$$\mathcal{D}_{rB}(\chi_M) = \chi_{\mathcal{D}_{rB}(M)} \text{ and } \mathcal{E}_{rB}(\chi_M) = \chi_{\mathcal{E}_{rB}(M)}. \tag{4.10}$$

The opening and closing of $\rho : \mathbb{R}^d \to [0,1]$ are defined by expressions (4.5) and (4.6), and these operators are idempotent and satisfy the ordering

$$\mathcal{O}_{rB}(\mathcal{O}_{rB}(\rho))(x) = \mathcal{O}_{rB}(\rho)(x) \leq \rho(x) \leq \mathcal{C}_{rB}(\rho)(x) = \mathcal{C}_{rB}(\mathcal{C}_{rB}(\rho))(x) \tag{4.11}$$

for any $x \in \mathbb{R}^d$.

In computational topology optimization, it is natural to consider (relaxed indicator) functions $\rho : \Omega \to [0,1]$ on bounded and convex design domains $\Omega \subset \mathbb{R}^d$. In this case, definitions (4.8) and (4.9) cannot be applied directly since ρ is undefined in $\Omega^\complement$. To resolve this issue, we may apply definitions (4.8) and (4.9) on some extension $\tilde{\rho} : \mathbb{R}^d \to [0,1]$ of $\rho : \Omega \to [0,1]$. As is discussed briefly in Publication III, it may even be beneficial to tune the extension to the problem at hand. Another possibility is to modify definitions (4.8) and (4.9) to directly handle $\rho : \Omega \to [0,1]$,

$$\mathcal{D}_{rB}^{\Omega}(\rho)(x) \coloneqq \sup_{y \in (x+rB)\cap\Omega} \rho(y), \tag{4.12}$$

$$\mathcal{E}_{rB}^{\Omega}(\rho)(x) \coloneqq \inf_{y \in (x+rB)\cap\Omega} \rho(y). \tag{4.13}$$

In Publication III, we study operations (4.12)–(4.13), the corresponding operations on sets $M \subset \Omega$, and introduce the minimum length scale

$$R_B^{\Omega}(M) \coloneqq \inf_{x \in M} \sup\{r > 0 \mid \exists m \in M \text{ s.t. } x \in (m + rB) \cap \Omega \subset M\} \tag{4.14}$$

for $M \subset \Omega$. Formally, $R_B^{\mathbb{R}^d}(M) = R_B(M)$, where $R_B(M)$ is defined by expression (4.1). The opening and closing of $\rho : \Omega \to [0,1]$ are defined in analogy with definitions (4.5) and (4.6), and these operators are idempotent and satisfy an ordering analogous to ordering (4.11). The main theoretical result of Publication III is Theorem 3, which demonstrates that, for any nonempty $M \subset \Omega$,

$$R_B^{\Omega}(M) = \sup\{r > 0 \mid \chi_M = \mathcal{O}_{rB}^{\Omega}(\chi_M)\}. \tag{4.15}$$

Note that the condition $\chi_M = \mathcal{O}_{rB}^{\Omega}(\chi_M)$ only holds for particular combinations of sets M and radii r, in contrast to $\chi_M \leq \mathcal{O}_{rB}^{\Omega}(\chi_M)$, which always holds. Characterization (4.15) not only establishes a connection between the minimum length scale (4.14) and the morphological operations (4.12) and (4.13), but also provides a computational foundation for estimation of minimum length scales using morphological operators.

For the discretized topology optimization problem, we consider morphological operations on design vectors $\boldsymbol{\rho} \in [0,1]^n$ defined by

$$\mathcal{D}_i(\boldsymbol{\rho}) \coloneqq \max_{j \in \mathcal{N}_i} \rho_j, \tag{4.16}$$

$$\mathcal{E}_j(\boldsymbol{\rho}) \coloneqq \min_{j \in \mathcal{N}_i} \rho_j, \tag{4.17}$$

where the neighborhood of element i, with centroid $x_i \in \Omega$, is defined as

$$\mathcal{N}_i = \{j \mid x_j - x_i \in rB\}. \tag{4.18}$$

To ease the notation, the dependence on the structuring element rB and the domain Ω of the morphological operations (4.16) and (4.17) has been suppressed. Note that the symmetry $rB = -rB$ implies that the collection of neighborhoods is symmetric, that is, for any pair of elements i, j,

$$j \in \mathcal{N}_i \text{ implies } i \in \mathcal{N}_j. \tag{4.19}$$

The opening and closing of $\boldsymbol{\rho}$ are defined in analogy with definitions (4.5) and (4.6), and these operators are idempotent and satisfy an ordering analogous to ordering (4.11). The dilation (4.16) and erosion (4.17) satisfy

$$\mathbf{1}_{\boldsymbol{n}} - \boldsymbol{\mathcal{E}}(\boldsymbol{\rho}) = \boldsymbol{\mathcal{D}}(\mathbf{1}_{\boldsymbol{n}} - \boldsymbol{\rho}), \tag{4.20}$$

which is analogous to complementarity relation (4.4). Moreover, any morphological operator—dilate, erode, open, or close—maps $\boldsymbol{\rho} \in \{0,1\}^n$ to $\{0,1\}^n$. Appealing to expression (4.15), we say that the minimum length scale (relative B) of the material phase represented by $\rho_i = 1$ of $\mathbf{0} \neq \boldsymbol{\rho} \in \{0,1\}^n$ is at least $r > 0$ if and only if

$$\boldsymbol{\rho} = \boldsymbol{\mathcal{O}}(\boldsymbol{\rho}). \tag{4.21}$$

Similarly, we say that the minimum length scale (relative B) of the material phase represented by $\rho_i = 0$ of $\mathbf{1}_{\boldsymbol{n}} \neq \boldsymbol{\rho} \in \{0,1\}^n$ is at least $r > 0$ if and only if

$$\mathbf{1}_{\boldsymbol{n}} - \boldsymbol{\rho} = \boldsymbol{\mathcal{O}}(\mathbf{1}_{\boldsymbol{n}} - \boldsymbol{\rho}), \tag{4.22}$$

which by complementarity (4.20) is equivalent to

$$\boldsymbol{\rho} = \boldsymbol{\mathcal{C}}(\boldsymbol{\rho}). \tag{4.23}$$

Thus the minimum length scale of each of the two phases of material of a design $\boldsymbol{\rho} \in \{0,1\}^n$ that satisfies $\mathbf{0} \neq \boldsymbol{\rho} \neq \mathbf{1}_{\boldsymbol{n}}$ is at least $r > 0$ if and only if

$$\boldsymbol{\mathcal{O}}(\boldsymbol{\rho}) = \boldsymbol{\mathcal{C}}(\boldsymbol{\rho}). \tag{4.24}$$

We note that it is possible to consider *different* minimum length scales on the two phases of material by replacing expression (4.24) with

$$\boldsymbol{\mathcal{O}}_{rB}(\boldsymbol{\rho}) = \boldsymbol{\mathcal{C}}_{r'B'}(\boldsymbol{\rho}), \tag{4.25}$$

where $r' > 0$ and B' is the open unit ball of some norm on $\mathbb{R}^d$.

The idempotence of the open operator implies that condition (4.21) is fulfilled if $\boldsymbol{\rho} = \boldsymbol{\mathcal{O}}(\hat{\boldsymbol{\rho}})$ for some $\hat{\boldsymbol{\rho}} \in [0,1]^n$, while the idempotence of the close operator implies that condition (4.23) holds if $\boldsymbol{\rho} = \boldsymbol{\mathcal{C}}(\hat{\boldsymbol{\rho}})$ for some $\hat{\boldsymbol{\rho}} \in [0,1]^n$. In fact, it is sufficient that $\boldsymbol{\rho} = \boldsymbol{\mathcal{D}}(\hat{\boldsymbol{\rho}})$ or $\boldsymbol{\rho} = \boldsymbol{\mathcal{E}}(\hat{\boldsymbol{\rho}})$ to guarantee fulfillment of condition (4.21) or (4.23), respectively. Therefore, introducing $\boldsymbol{F}(\boldsymbol{\rho}) = \boldsymbol{\mathcal{D}}(\boldsymbol{\rho})$ or $\boldsymbol{F}(\boldsymbol{\rho}) = \boldsymbol{\mathcal{O}}(\boldsymbol{\rho})$ as a filter in the formulation of a discretized density based topology optimization problem, such as the minimum compliance problem, imposes a minimum size on the material phase represented by 1, while $\boldsymbol{F}(\boldsymbol{\rho}) = \boldsymbol{\mathcal{E}}(\boldsymbol{\rho})$ or $\boldsymbol{F}(\boldsymbol{\rho}) = \boldsymbol{\mathcal{C}}(\boldsymbol{\rho})$ imposes a minimum size on the phase represented by 0. Unfortunately, formulations involving (exact) morphological operators, which are non-differentiable, are incompatible with the efficient gradient-based optimization algorithms preferred to solve large-scale design optimization problems. However, Sigmund—who appears to have been the first to recognize the potential of mathematical morphology to impose minimum length scales in (gradient based) topology optimization problems—avoids the issue by introducing differentiable density filters that approximate morphological operators [53]. As can be seen in the next chapter, many filters introduced for topology optimization can be interpreted as differentiable approximations of morphological operators. Note that, for the purpose of imposing minimum length scale, filters need to

provide accurate approximation of morphological operators for binary $\boldsymbol{\rho} \in \{0,1\}^n$ only. To ease the presentation of filters in the next chapter, we introduce the following definition.

Definition 1. A parametrized family of filters $\boldsymbol{F}_\alpha : [0,1]^n \to [0,1]^n$, $\alpha > 0$ is a *differentiable approximation on* $\{0,1\}^n$ of a morphological operator $\boldsymbol{\mathcal{M}}$ if and only if $\boldsymbol{F}_\alpha$ is differentiable for each $\alpha > 0$, and there is a filter $\boldsymbol{F} : [0,1]^n \to [0,1]^n$ such that

$$\begin{aligned} \boldsymbol{F}(\boldsymbol{\rho}) &= \boldsymbol{\mathcal{M}}(\boldsymbol{\rho}) \quad \text{for each } \boldsymbol{\rho} \in \{0,1\}^n, \\ \lim_{\alpha \to 0} \boldsymbol{F}_\alpha(\boldsymbol{\rho}) &= \boldsymbol{F}(\boldsymbol{\rho}) \quad \text{for each } \boldsymbol{\rho} \in [0,1]^n. \end{aligned} \tag{4.26}$$

5. Density filters

5.1 The linear filter

The simplest filter observed to resolve the mesh-dependency issue is the linear (density) filter

$$\boldsymbol{F}(\boldsymbol{\rho}) = \boldsymbol{W}\boldsymbol{\rho}, \tag{5.1}$$

where $\boldsymbol{W} = [w_{ij}] \in \mathbb{R}^{n\times n}$ is a matrix containing non-negative normalized weights,

$$\boldsymbol{W}\mathbf{1}_{\boldsymbol{n}} = \mathbf{1}_{\boldsymbol{n}}, \tag{5.2a}$$

$$w_{ij} \in [0, 1). \tag{5.2b}$$

Note that condition (5.2b) excludes the trivial filter $\boldsymbol{\rho} \mapsto \boldsymbol{\rho}$. In topology optimization, it is customary to first introduce a neighborhood shape $\mathbb{R}^d \supset \mathcal{N} \ni 0$ that is independent of the partition of the design domain, and define the neighborhood of element i by

$$\mathcal{N}_i \coloneqq \{j \mid x_j - x_i \in \mathcal{N}\}, \tag{5.3}$$

where x_i denotes the centroid of element i. Second, w_{ij} are determined so that properties (5.2) hold and the neighborhood $\mathcal{N}_i$ consists precisely of those elements j such that $w_{ij} > 0$. We note that for a given neighborhood shape, the behavior of the weights can be chosen in a multiple of ways. Note also that if $\mathcal{N} = rB$, the definitions (5.3) and (4.18) coincide. Unless otherwise stated, we assume that the collection of neighborhoods is symmetric in the sense of property (4.19).

The linear filter (5.1), which was introduced in topology optimization by Bruns & Tortorelli [18], is the core element of all filters used in topology optimization. Popular implementations of the linear filter have ball-shaped neighborhoods of a given radius with weights that are uniform or decay linearly from the neighborhood center. The radius of the ball-shaped neighborhoods is often referred to as the filter radius. Intuitively, the linear filter handles the mesh-dependency issue by smearing out details smaller than the neighborhood. The main drawback of the linear filter is that it prevents sharp transitions between regions where $\rho_i = 0$ and $\rho_i = 1$. More recently, mesh-independent designs with almost sharp transitions between regions where $\rho_i = 0$ and $\rho_i = 1$ have been observed for a range of *nonlinear* filters [53, 59].

Before continuing with nonlinear filters, we describe a linear filtering algorithm devised by Lazarov & Sigmund [41]. The solution $F(\rho)$ to the elliptic boundary value problem

$$\begin{aligned} -a^2\Delta F(\rho) + F(\rho) &= \rho \quad \text{in } \Omega, \\ n \cdot \nabla F(\rho) &= 0 \quad \text{on } \partial\Omega, \end{aligned} \tag{5.4}$$

may be represented as the convolution of ρ with a positive and normalized Green's function, and where $a \neq 0$ controls the decay of the Green's function. However, instead of explicitly discretizing the convolution, which directly leads to an expression of the form (5.1), we evaluate the filter by solving a finite element (or finite

volume) discretization of the boundary value problem (5.4). Note that the finite element approximation of $F(\rho)$ will not be piecewise constant, even if ρ is assumed to be piecewise constant.

5.2 Nonlinear filters

One of the main contributions of Publication I is the introduction of the class of generalized fW-mean filters, which contains most filters in the literature on topology optimization. Generalized fW-mean filters have the form

$$\boldsymbol{F}(\boldsymbol{\rho}) = \boldsymbol{g}\left(\boldsymbol{W}\boldsymbol{f}(\boldsymbol{\rho})\right), \tag{5.5}$$

where $f, g : [0,1] \to [0,1]$ are continuous and surjective. Note that expression (5.5) is a discrete analogue of expression (3.21). Moreover, note that requiring $[0,1]$ to be the range of f and the domain of g is superfluous. Indeed, let $b > a$, and assume that $\hat{f} : [0,1] \to [a,b]$ and $\hat{g} : [a,b] \to [0,1]$ are continuous and surjective, then $f, g : [0,1] \to [0,1]$ defined by

$$\begin{aligned} f(x) &= \frac{\hat{f}(x) - a}{b - a}, \\ g(x) &= \hat{g}\big((b-a)x + a\big) \end{aligned} \tag{5.6}$$

are continuous and surjective, and

$$\boldsymbol{g}\left(\boldsymbol{W}\boldsymbol{f}(\boldsymbol{\rho})\right) = \hat{\boldsymbol{g}}\left(\boldsymbol{W}\hat{\boldsymbol{f}}(\boldsymbol{\rho})\right) \tag{5.7}$$

for any $\boldsymbol{\rho} \in [0,1]^n$. We define the fW-mean filters as the subclass of the generalized fW-mean filters realized by requiring f to be bijective and $g = f^{-1}$,

$$\boldsymbol{F}(\boldsymbol{\rho}) = \boldsymbol{f}^{-1}\left(\boldsymbol{W}\boldsymbol{f}(\boldsymbol{\rho})\right). \tag{5.8}$$

That is, $F_i(\boldsymbol{\rho})$ is a (weighted) quasi arithmetic mean [39, 45], also known as the (weighted) f-mean,

$$F_i(\boldsymbol{\rho}) = f^{-1}\left(\sum_{j \in \mathcal{N}_i} w_{ij} f(\rho_j)\right) \iff f(F_i(\boldsymbol{\rho})) = \sum_{j \in \mathcal{N}_i} w_{ij} f(\rho_j). \tag{5.9}$$

In fact, to the best of our knowledge, only bijective f and $g = h \circ f^{-1}$, where $h : [0,1] \to [0,1]$ is continuous, surjective and increasing, appear in the literature on topology optimization; that is,

$$\boldsymbol{F}(\boldsymbol{\rho}) = \boldsymbol{h}\left(\boldsymbol{f}^{-1}\left(\boldsymbol{W}\boldsymbol{f}(\boldsymbol{\rho})\right)\right). \tag{5.10}$$

The Heaviside filter [31], which consists of applying a particular approximation of the Heaviside step function to the linear filter, is given by formula (5.5) with

$$\begin{aligned} f(x) &= x, \\ g(x) &= 1 - e^{-\beta x} + e^{-\beta} x. \end{aligned} \tag{5.11}$$

The parameter $\beta \geq 0$ controls the sharpness of the step. For $\beta = 0$ the Heaviside filter is nothing but the linear filter (5.1), and when $\beta \to \infty$ the Heaviside filter approaches

$$F_i(\boldsymbol{\rho}) = \begin{cases} 0 & \text{if } \rho_j = 0 \text{ for all } j \in \mathcal{N}_i, \\ 1 & \text{otherwise.} \end{cases} \tag{5.12}$$

Wang et al. [62] introduced a different approximation of the Heaviside step function with variable step location $\eta \in [0, 1]$ and thereby obtained a variation of the Heaviside filter given by formula (5.5) with

$$\begin{aligned} f(x) &= x, \\ g(x) &= \frac{\tanh(\beta\eta) + \tanh\left(\beta(x - \eta)\right)}{\tanh(\beta\eta) + \tanh\left(\beta(1 - \eta)\right)}. \end{aligned} \tag{5.13}$$

We refer to this variation of the Heaviside filter as the $\tanh$-filter. Similarly as for the Heaviside filter, the parameter $\beta > 0$ controls the sharpness of the step, and the linear filter is retrieved in the limit $\beta \to 0$, since $g(x)$ in definition (5.13) tends to x. When $\beta \to \infty$ and $\eta \in (0, 1)$, $g(x)$ in definition (5.13) tends to

$$\begin{cases} 0 & \text{if } x < \eta, \\ 1/2 & \text{if } x = \eta, \\ 1 & \text{if } x > \eta. \end{cases} \tag{5.14}$$

As pointed out by Sigmund [53], both the Heaviside filter (5.11) and the $\tanh$-filter (5.13) are differentiable approximations on $\{0, 1\}^n$ of the dilate operator (4.16) in the limit $\beta \to \infty$ (Definition 1 with $\alpha \coloneqq 1/\beta$).

The exponential dilate filter [53], which is given by formula (5.5) with

$$\begin{aligned} f(x) &= e^{\beta x}, \\ g(x) &= f^{-1}(x) = \frac{1}{\beta} \ln x, \end{aligned} \tag{5.15}$$

where $\beta \in (0, \infty)$, was introduced as a differentiable approximation of the dilate operator (4.16), that is,

$$\lim_{\beta \to \infty} \frac{1}{\beta} \mathbf{ln}\left(\boldsymbol{W} \boldsymbol{e}^{\beta \boldsymbol{\rho}}\right) = \boldsymbol{\mathcal{D}}(\boldsymbol{\rho}) \tag{5.16}$$

for any $\boldsymbol{\rho} \in [0, 1]^n$. Analogously, the exponential erode filter [53], which is given by formula (5.5) with

$$\begin{aligned} f(x) &= e^{-\beta x}, \\ g(x) &= f^{-1}(x) = -\frac{1}{\beta} \ln x, \end{aligned} \tag{5.17}$$

is a differentiable approximation of the erode operator (4.16), that is,

$$\lim_{\beta \to \infty} -\frac{1}{\beta} \mathbf{ln}\left(\boldsymbol{W} \boldsymbol{e}^{-\beta \boldsymbol{\rho}}\right) = \boldsymbol{\mathcal{E}}(\boldsymbol{\rho}) \tag{5.18}$$

for any $\boldsymbol{\rho} \in [0,1]^n$. Both the exponential dilate and the exponential erode filter approach the linear filter (5.1) when $\beta \to 0$. The exponential dilate and exponential erode filters satisfy

$$\mathbf{1_n} - \left(-\frac{1}{\beta}\mathbf{ln}\left(\boldsymbol{W}\boldsymbol{e}^{-\beta\boldsymbol{\rho}}\right)\right) = \frac{1}{\beta}\mathbf{ln}\left(\boldsymbol{W}\boldsymbol{e}^{\beta(\mathbf{1_n}-\boldsymbol{\rho})}\right), \tag{5.19}$$

which is the analogue of the complementarity relation (4.20).

In general, complementarity is a basis for generating new filters from existing filters [59]. Indeed, if $\tilde{\boldsymbol{F}}$ is the generalized fW-mean filter (5.5) defined by $\tilde{f}$ and $\tilde{g}$, then the complementary filter

$$\boldsymbol{F}(\boldsymbol{\rho}) \coloneqq \mathbf{1_n} - \tilde{\boldsymbol{F}}(\mathbf{1_n} - \boldsymbol{\rho}) \tag{5.20}$$

is the generalized fW-mean filter (5.5) defined by $f(x) \coloneqq \tilde{f}(1-x)$ and $g(x) = 1 - \tilde{g}(x)$, and

$$\mathbf{1_n} - \boldsymbol{F}(\boldsymbol{\rho}) = \tilde{\boldsymbol{F}}(\mathbf{1_n} - \boldsymbol{\rho}) \tag{5.21}$$

by construction. Let $\tilde{\boldsymbol{F}}_\alpha, \boldsymbol{F}_\alpha$ be parametrized families of filters that satisfy the complementarity relation (5.21) for each $\alpha > 0$. Then $\boldsymbol{F}_\alpha(\boldsymbol{\rho}) \to \boldsymbol{\mathcal{E}}(\boldsymbol{\rho})$ ($\boldsymbol{\mathcal{D}}(\boldsymbol{\rho})$) for some $\boldsymbol{\rho} \in [0,1]^n$ as $\alpha \to 0$ if and only if $\tilde{\boldsymbol{F}}_\alpha(\mathbf{1_n} - \boldsymbol{\rho}) \to \boldsymbol{\mathcal{D}}(\mathbf{1_n} - \boldsymbol{\rho})$ ($\boldsymbol{\mathcal{E}}(\mathbf{1_n} - \boldsymbol{\rho})$) as $\alpha \to 0$. Therefore, the complementary filters (5.20) to the Heaviside-filter (5.11) and the $\tanh$-filter (5.13) are differential approximations on $\{0,1\}^n$ of the erode operator (4.17).

Svanberg & Svärd [59] introduced filters based on the harmonic and geometric means. The harmonic erode filter, defined by

$$\begin{aligned} f(x) &= \frac{1}{x+\alpha}, \\ g(x) &= f^{-1}(x) = \frac{1}{x} - \alpha, \end{aligned} \tag{5.22}$$

and the geometric erode filter, defined by

$$\begin{aligned} f(x) &= \ln(x+\alpha), \\ g(x) &= f^{-1}(x) = e^x - \alpha, \end{aligned} \tag{5.23}$$

where $\alpha > 0$, are differentiable approximations on $\{0,1\}^n$ of the erode operator (4.17). In the limit $\alpha \to \infty$, both the harmonic erode and geometric erode filters approach the linear filter (5.1). The harmonic dilate and geometric dilate filters are defined to be complementary (5.20) to the harmonic erode and geometric erode filters, respectively.

New filters may also be constructed by composing existing filters [53]. In particular, by composing differential approximations of the dilate operator (4.16) and the erode operator (4.17), we may obtain differential approximations of the open and close operators. For instance, the exponential open and close filters [53] are formed in this way by composing the exponential filters defined by the functions (5.15) and (5.17). In an attempt to impose minimum length scales on both material phases, Sigmund [53] introduced the exponential open-close and close-open filters by composing the exponential open and exponential close. Although such filters have been observed to provide designs with minimum length scales on both material phases [53], this cannot be guaranteed in general [52].

For each element i the bilateral density filter [63] is defined by

$$F_i(\boldsymbol{\rho}) = \frac{\sum\limits_{j \in \mathcal{N}_i} w_{ij} \tilde{w}(|\rho_i - \rho_j|)\rho_j}{\sum\limits_{j \in \mathcal{N}_i} w_{ij} \tilde{w}(|\rho_i - \rho_j|)}, \tag{5.24}$$

where $\tilde{w} : [0,1] \to (0,\infty)$ is non-increasing and provides weighting depending on the distance $|\rho_i - \rho_j|$, in contrast to w_{ij}, which provides weighting depending on the distance between element centroids $|x_i - x_j|$. We note that the bilateral filter (5.24) is not of the form (5.5).

Another type of filters not of the form (5.5) are so-called combination filters [53] defined by

$$\boldsymbol{F}(\boldsymbol{\rho}) = \frac{1}{2}\left(\boldsymbol{\mathcal{O}}_\alpha(\boldsymbol{\rho}) + \boldsymbol{\mathcal{C}}_\alpha(\boldsymbol{\rho})\right), \tag{5.25}$$

where $\boldsymbol{\mathcal{O}}_\alpha$ and $\boldsymbol{\mathcal{C}}_\alpha$ denote differentiable approximations of the open and close operators, respectively. Note that if $a, b \in [0,1]$ and $(a+b)/2 \in \{0,1\}$, then $a = b \in \{0,1\}$. Thus, if $\boldsymbol{F}$ is a combination filter (5.25) and $\boldsymbol{\rho} \in [0,1]^n$ is such that $\boldsymbol{F}(\boldsymbol{\rho}) \in \{0,1\}^n$, then $\boldsymbol{\mathcal{O}}_\alpha(\boldsymbol{\rho}) = \boldsymbol{\mathcal{C}}_\alpha(\boldsymbol{\rho}) \in \{0,1\}^n$. Appealing to condition (4.24), we find that the combination filters (5.25) are suitable candidates for providing minimum length scales on both material phases.

It is interesting to compare the computational cost of the filter to that of solving the linear system (3.25), which may be reduced to $O(n)$ by applying a properly tuned multigrid method. Since the functions f and g are applied pointwise, the computational complexity of evaluating any generalized fW-mean filter is controlled by the computational complexity of averaging over the neighborhoods. In fact, to evaluate any of the filters presented in this section, we need to compute averages over the neighborhoods, that is, to evaluate the linear filter (5.1). For a general set of weights w_{ij}, the computational cost of evaluating the linear filter is proportional to $\sum_{j=1}^n |\mathcal{N}_j|$, where $|\mathcal{N}_i|$ denotes the number of neighbors to element i. Recall that in topology optimization, the neighborhoods are typically defined by a neighborhood shape $\mathcal{N}$ that is independent of the partitioning of the design domain Ω. In this case $\mathcal{N}_i = O(n)$, and thus the computational cost of evaluating the linear filter is $O(n^2)$. Nevertheless, for particular sets of weights and neighborhood shapes the computational cost can be reduced. If $w_{ij} = w(i-j)$, for some compactly supported non-negative function w, the linear filter (5.1) corresponds to a convolution that can be efficiently evaluated by the FFT (Fast Fourier Transform), which has (asymptotic) computational complexity $O(n \log n)$. To evaluate filters in topology optimization by the FFT appears to have been first proposed by Lazaraov & Wang [42]. In case the weights are uniform, $w_{ij} = |\mathcal{N}_i|^{-1}$, and the neighborhood shape is polytopal, the linear filter can be evaluated in $O(n)$ operations. This was first established in the context of image analysis ($d = 2$) for octagonal neighborhoods by Glasbey & Jones [28] and later extended to general polygonal neighborhoods by Sun [56]. The basic idea behind the $O(n)$ algorithms is to compute sums by an update scheme,

$$\sum_{k \in \mathcal{N}_i} = \sum_{k \in \mathcal{N}_j} + \sum_{k \in \mathcal{N}_i \setminus \mathcal{N}_j} - \sum_{k \in \mathcal{N}_j \setminus \mathcal{N}_i}, \tag{5.26}$$

which can be performed recursively since the facets of a (convex) d-dimensional polytope are (convex) $(d-1)$-dimensional polytopes. In Publication I, we present

an $O(n)$ algorithm for summation over rhombicuboctahedral neighborhoods in 3D. Moreover, we demonstrate that the computational complexity, for a fixed Cartesian partition of Ω, is essentially independent of the size of the rhombicuboctahedral neighborhoods. In Publication II, we note that some *non-uniformly* weighted linear filters can be constructed by sequentially applying *uniformly* weighted linear filters. In particular, if the weight matrix $\boldsymbol{W}$ (5.2) encodes uniform weights on neighborhoods defined by a convex neighborhood shape $\mathcal{N} \ni 0$, then $\boldsymbol{W}^2$ encodes weights that decay from the neighborhood center of neighborhoods defined by the neighborhood shape $2\mathcal{N}$. Note that the linear filter defined as a finite element solution to boundary value problem (5.4) can be evaluated in $O(n)$ operations by applying a properly tuned multi-grid solver [41].

To apply gradient-based optimization algorithms to solve topology optimization problems involving filters, we need to evaluate the filter gradients. By the chain rule, the additional computational cost attributable to the filter (compare expression (3.40) with expression (3.35); (3.38) with (3.31)) corresponds to the evaluation of

$$\sum_{i=1}^{n} v_i \frac{\partial F_i}{\partial \rho_j} = (\boldsymbol{J}^T \boldsymbol{v})_j \tag{5.27}$$

for some $\boldsymbol{v} \in \mathbb{R}^n$, where $\boldsymbol{J} \coloneqq [\partial F_i / \partial \rho_j] \in \mathbb{R}^{n \times n}$ denotes the Jacobian of $\boldsymbol{F}$. We note that expression (5.27) may be interpreted as a linear filtering of $\boldsymbol{v}$ where the weights are given by the transpose of the Jacobian. In Publication II, we demonstrate that for (a sequence of) fW-mean filters (5.8) with uniform weights over symmetric polytopal neighborhoods, expression (5.27) can be evaluated by the same $O(n)$ algorithm used to evaluate the filter.

We conclude by noting that if $\boldsymbol{F}$ is a fW-mean filter for some differentiable function f with $f' \neq 0$, then by differentiating expression (5.8),

$$\frac{\partial F_i}{\partial \rho_j} = w_{ij} \frac{f'(\rho_j)}{f'(F_i(\boldsymbol{\rho}))} \geq 0; \tag{5.28}$$

that is, property (3.41) holds. In fact, property (3.41) continues to hold if the filter is given by expression (5.10) for some differentiable h with $h' > 0$, which is true for all generalized fW-mean filters presented in this section.

6. Design of coaxial-to-waveguide transitions

Coaxial cables and rectangular waveguides, which are routinely applied to transmit electromagnetic signals between various devices, have fundamentally different transmission characteristics. Therefore, transitions between coaxial cables and rectangular waveguides need to be carefully designed to assure proper transmission of signals, without excessive reflections and losses, which may cause overheating. Since it is well beyond the scope of this thesis to give a comprehensive review of the literature on the design of electromagnetic devices, we refer the interested reader to the dissertation by Hassan [33] and to the references therein. The presentation here is tuned towards Publication IV, which demonstrates the applicability of the generalized fW-mean filter framework in a challenging engineering design problem. We note that the main contribution of Hägg to Publication IV concerns the construction and implementation of the filters employed in the two-phase continuation approach described below.

Figure 7 illustrates the setup considered in Publication IV for optimizing a so-called end-launcher transition in which a coaxial cable is connected at the rear end of a rectangular waveguide. The idea is to optimize the layout of (a very thin layer of) conducting material (metal) in the planar design domain $\Omega \subset \mathbb{R}^2$, which is in contact with the center conductor of the coaxial cable and sits on top of a low-loss dielectric substrate that extends all the way to the rear wall of the waveguide, so that proper transmission of signals is achieved for a band of frequencies. As described by Hassan et al. [34], the resulting designs can be manufactured by photoengraving a metal-coated dielectric substrate. Assuming that the coaxial cable and the rectangular waveguide contain only linear isotropic media, the evolution of the electric field

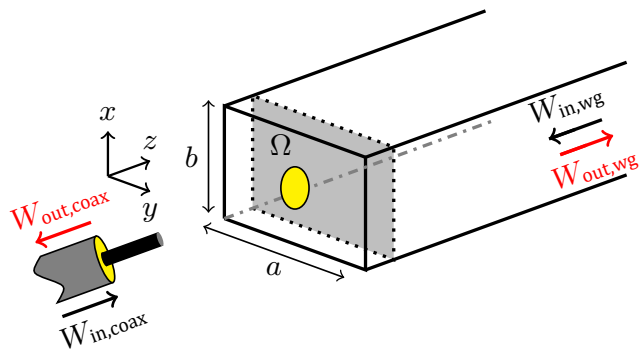

Figure 7: End-launcher transition. A coaxial cable is connected at the rear end of a rectangular waveguide. The layout of conducting material in Ω is to be determined so that signals are properly transmitted.

E and the magnetic field H is modeled by Maxwell's equations

$$\partial_t \mu H + \nabla \times E = 0, \tag{6.1a}$$

$$\partial_t \epsilon E + \sigma E - \nabla \times H = 0, \tag{6.1b}$$

where μ, ϵ, and σ denote the local permeability, permittivity, and conductivity of the medium. The inner conductor and shield of the coaxial cable, as well as the walls of the rectangular waveguide, are assumed to be perfectly conducting. For computational reasons, the coaxial cable is truncated to finite length using a non-reflecting boundary condition, which also provides a mean to introduce signals in the coaxial cable, while the rectangular waveguide is truncated to finite length using a perfectly matched layer. The band of frequencies for which the transition is optimized is chosen between the first and second cutoff frequencies of the rectangular waveguide, so that all modes, except for the so-called TE_{10} mode, are evanescent [37, § 8]. A total-field/scattered-field technique is employed to introduce signals in the rectangular waveguide.

The effect of different layouts of material within the design domain is captured in equation (6.1b) by a heterogeneous conductivity distribution that is allowed to take values in a prespecified range $[\underline{\sigma}, \overline{\sigma}] \subset (0, \infty)$. Similarly as for the minimum compliance and the minimum "heat compliance" problems, we introduce a design variable field $p : \Omega \to [0, 1]$ to parametrize the conductivity distribution[1]. To accommodate for the vastly different conductivities of bad compared to good conductors, we introduce the parametrization

$$\sigma(p) = \underline{\sigma} e^{\gamma p} \text{ within } \Omega, \tag{6.2}$$

where $\gamma > 0$ is a prespecified parameter. For instance, in Publication IV, $\underline{\sigma} = 10^{-3}$ S/m and $\gamma = 8 \ln 10$ are used, so $\overline{\sigma} = \underline{\sigma} e^{\gamma} = 10^5$ S/m.

We choose the finite-difference time-domain method (FDTD) to generate numerical solutions to Maxwell's equations (6.1). The conductivity is then evaluated at the edge-centers of so-called cubical Yee cells that constitute a Cartesian partition of the computational domain. Therefore, similarly as in the previous chapters, it is natural to represent the design by a design vector $\boldsymbol{p} \in [0, 1]^n$, where n denotes the number of Yee cell edges within the design domain Ω.

For signals of finite duration, vanishing initial conditions, and for sufficiently long integration times, we have the energy balance

$$W_{\text{in,coax}} + W_{\text{in,wg}} = W_{\text{out,coax}} + W_{\text{out,wg}} + W_{\text{loss}}, \tag{6.3}$$

where $W_{\text{in,coax}}$ and $W_{\text{in,wg}}$ denote incoming, and $W_{\text{out,coax}}$ and $W_{\text{out,wg}}$ outgoing energies in the coaxial cable and rectangular waveguide, respectively, and W_{loss} the Ohmic loss in the dielectric substrate and in the design domain Ω. To optimize the design of the transition, Publication IV introduces the objective function

$$J(\boldsymbol{p}) = \log \left(\frac{W_{\text{out,coax}}|_{W_{\text{in,wg}}}}{W_{\text{out,coax}}|_{W_{\text{in,coax}}}} \right), \tag{6.4}$$

[1] The reason to denote the design field by p, and not ρ, is to avoid confusion, as the latter often denotes the distribution of electric charge in the context of electrodynamics.

where $W_{\text{out,coax}}|_{W_{\text{in,wg}}}$ and $W_{\text{out,coax}}|_{W_{\text{in,coax}}}$ denote the outgoing energies in the coaxial cable when the system is fed through the waveguide or through the coaxial cable, respectively. Thus, to evaluate the objective function (6.4), Maxwell's equations (6.1) need to be solved twice with different feeds. Beware that Publication IV employs a *maximization* formulation, contrary to previous chapters that employ *minimization* formulations. Hence, the objective function (6.4) captures the intuitive desire to maximize the transmission ($W_{\text{out,coax}}|_{W_{\text{in,wg}}}$) of a signal fed through the waveguide and minimize the reflection ($W_{\text{out,coax}}|_{W_{\text{in,coax}}}$) of a signal fed through the coaxial cable. Note that due to reciprocity, there is no need to consider the transmission when the system is fed through the coaxial cable nor the reflection when the system is fed through the waveguide. On the one hand, energy balance (6.3) reveals that maximizing $W_{\text{out,coax}}|_{W_{\text{in,wg}}}$ for fixed $W_{\text{in,wg}}$ and vanishing $W_{\text{in,coax}}$ is equivalent to minimizing the sum $(W_{\text{out,wg}} + W_{\text{loss}})|_{W_{\text{in,wg}}}$. That is, the sum of the reflection and the loss is minimized in this case. On the other hand, energy balance (6.3) also reveals that minimizing $W_{\text{out,coax}}|_{W_{\text{in,coax}}}$ for fixed $W_{\text{in,coax}}$ and vanishing $W_{\text{in,wg}}$ is equivalent to maximizing the sum $(W_{\text{out,wg}} + W_{\text{loss}})|_{W_{\text{in,coax}}}$. That is, the sum of the transmission and the loss is maximized in this case—with the apparent risk of promoting designs with excessive loss. Nonetheless, the maximization of the combination of transmission and reflection embodied in objective function (6.4) was computationally found to produce designs exhibiting low loss and being almost exclusively consisting of the extreme conductivities $\underline{\sigma}$ and $\overline{\sigma}$. This natural penalization of intermediate values of the design variables induced by the objective function has its explanation in the fact that the limiting cases of a perfect electric conductor ($\sigma = \infty$) or a perfect electric insulator ($\sigma = 0$) are both lossless, and that the loss term W_{loss} for a given layout of material with homogeneous conductivity typically achieves a maximum for some value of the conductivity between the extremes $\underline{\sigma}$ and $\overline{\sigma}$. Contrary to the minimum compliance and the minimum "heat compliance" problems, there is therefore no need for explicit penalization of intermediate values of the design variables in this case.

This natural penalization of intermediate values of the design variables has, unfortunately, a tendency to make gradient based optimization algorithms to quickly converge to poorly performing local optima and may also prevent the transitioning between the extreme conductivities $\underline{\sigma}$ and $\overline{\sigma}$. To control the natural penalization, Hassan et al. [35] restricted the design vector to the image of a linear filter of the form (5.1) with disk-shaped neighborhoods of radius $R > 0$ by replacing occurrences of $\boldsymbol{p}$ in the problem formulation by $\boldsymbol{F}(\boldsymbol{p}) = \boldsymbol{W}\boldsymbol{p}$, which prevents sharp transitions between the extreme conductivities $\underline{\sigma}$ and $\overline{\sigma}$. Employing continuation over a sequence of decreasing filter radii, Hassan et al. [35] gradually removed the effect of the filter and obtained better performing low-loss designs. However, as demonstrated in Publication IV and seen in Figure 8a, the original continuation strategy of Hassan et al. [35] may produce designs containing small features, which are undesirable as they may increase losses as well as demands on the manufacturing accuracy. To counter also the formation of small features, Publication IV proposes a two phase continuation approach involving both linear and nonlinear filters. The first phase is a modification of the original continuation strategy of Hassan et al. [35] in which the filter radius of a linear filter is gradually decreased to a prespecified minimum radius $\underline{R}$. The second phase employs continuation over a sequence of decreasing val-

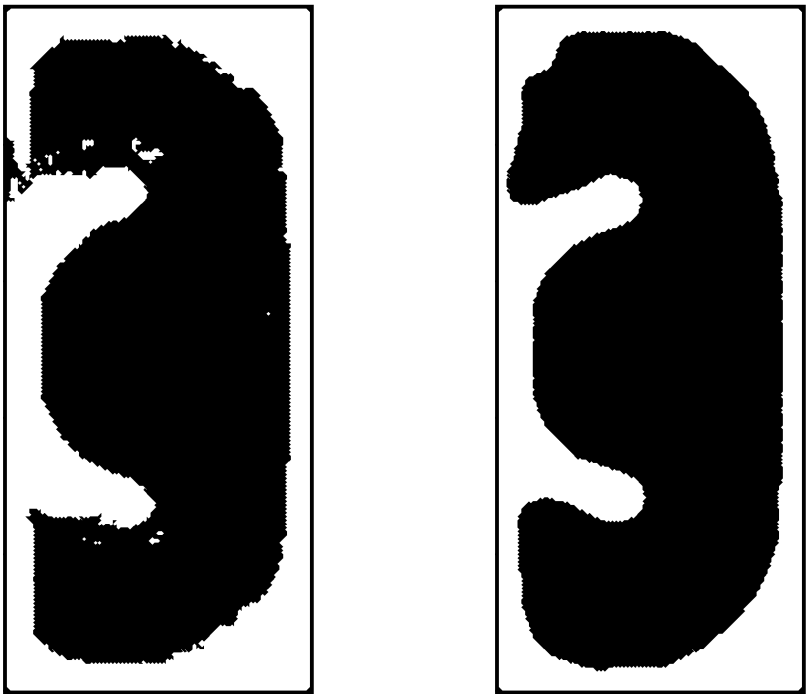

(a) (b)

Figure 8: Optimized designs of coaxial-to-waveguide transitions, where black represents the layout of highly conducting material to be distributed on dielectric substrates that are approximately 10×23 mm as illustrated by the bounding rectangles. (a) Design exhibiting undesirably small features obtained by the original one phase continuation strategy. (b) Design free of small features obtained by the proposed two-phase continuation strategy.

ues of the filter parameter α of a harmonic open-close filter with disk-shaped neighborhoods of fixed radius $\underline{R}$. Thus, the first phase is designed to control the natural penalization, while the second phase should counter the formation of small features while allowing for designs that are (almost) exclusively made of materials with the extreme conductivities $\underline{\sigma}$ and $\overline{\sigma}$. The computations in Publication IV involving the two phase continuation approach employs a streamlined implementation in which the first phase employs a harmonic open-close filter with sufficiently large parameter α to approximate a linear filter. Figure 8b displays an optimized design for which the proposed two phase continuation strategy successfully prevented the formation of small features.

As a measure to improve the performance of the optimized transitions further, Publication IV extends the freedom of design by stacking multiple layers of dielectric substrates supporting heterogeneous conductivity distributions that all are subject to simultaneous optimization.

7. Summary of publications: Part I

In **Publication I**, we introduce the class of generalized fW-mean filters (5.5), based on the concept of quasi-arithmetic mean, and develop some basic properties of such filters. Moreover, we demonstrate that there are $O(n)$ algorithms, based on updating scheme (5.26), for the evaluation of generalized fW-mean filters with uniform weights over polytopal neighborhoods. In particular, we explicitly provide an $O(n)$ algorithm for summing over rhombicuboctahedral neighborhoods, which can be seen as an extension to 3D of previously known 2D summation algorithms. We present numerical experiments to verify the claims on the computational complexity, as well as to illustrate the potential loss of element-wise accuracy when the range of numbers to be summed by the computer is large.

In **Publication II**, we prove existence of a global minimizer for an infinite dimensional fW-mean filtered penalized minimum compliance problem. We elaborate on general requirements of filters $\boldsymbol{F} : [0,1]^n \to [0,1]^n$, such as condition (3.37). Moreover, we demonstrate that *non-uniform* weighting on *complex* neighborhoods can be achieved by sequentially applying linear filters with *uniform* weights on *simple* neighborhoods. For instance, sequential application of two linear filters with uniform weights on square neighborhoods with a relative rotation of 45 degrees corresponds to a linear filter with non-uniform weights on octagonal neighborhoods. Furthermore, we build onto the framework of generalized fW-mean filters by detailing how to efficiently evaluate derivatives of generalized fW-mean filters, in particular for sequences of generalized fW-mean filters. In the final part of Publication II, we present numerical results for the penalized 2D minimum compliance and minimum "heat compliance" problems employing the $O(n)$ filtering algorithm for octagonal neighborhoods presented in Publication I to evaluate harmonic open-close filters.

In **Publication III**, we review methods for imposing minimum length scales in topology optimization. After a brief review on mathematical morphology on $\mathbb{R}^d$, we introduce a minimum length scale for subsets of a bounded convex domain $\Omega \subset \mathbb{R}^d$, introduce morphological operators on such subsets, and establish the connection between these morphological operators and the minimum length scale. We introduce conditions (4.21) and (4.23) to control the minimum length scale on the material phase represented by $\rho_i = 1$ and $\rho_i = 0$, respectively. Moreover, we introduce quality measures that quantify the residuals in conditions (4.21), (4.23), and (4.24). Inspired by the SIMP and RAMP approaches, we propose an approach for the minimum compliance problem and minimum "heat compliance" problem that promotes binary designs with minimum length scales on the two material phases by applying filters that approximate the morphological opening and closing. We present numerical results for both the minimum compliance problem and minimum "heat compliance" problem, compare different continuation schemes for the filter and penalty parameters, and explicitly estimate the minimum length scales of both material phases of the optimized designs.

In **Publication IV**, we develop a density based approach for optimizing the design of a transition that connects a coaxial cable to the rear end of a rectangular waveguide operating over a wide band of frequencies. The design domain consists of a plane (or a stack of a few separate planes) within the waveguide, located in the proximity of and parallel to the rear wall, and on which the layout of conducting material is to be determined as to achieve desirable performance. The idea of this setup is that the design may be realized by photoengraving of metal-coated dielectric substrates. The design optimization problem at hand suffers from two complications. First, there is a natural penalization of intermediate conductivities, which may lead gradient-based optimization algorithms to quickly converge to poorly performing local optima. Second, the optimized layouts may contain small features that are difficult to manufacture and may lead to excessive heating of the device. In Publication IV, these complications are addressed by introducing suitable filters in the problem formulation and employing a two-phase continuation strategy over filter parameters.

Part II
Analysis of Friedrichs Systems

8. Well-posedness of Friedrichs systems

In the beginning of the 20th century, Jacques Hadamard introduced the notion of well-posedness. An initial–boundary value problem is said to be well-posed in the sense of Hadamard if the following triad of properties holds [44, § 15.1]:

(i) The solution exists,

(ii) is unique, and

(iii) depends continuously on the data of the problem.

In property (iii), data collectively refers to initial data, boundary data, and source data. For problems originating from mathematical physics, property (i) asserts consistency of the model, (ii) reflects determinism of physical reality, and (iii) the frequent observation that similar circumstances lead to similar behaviors. A problem that lacks any of properties (i)–(iii) is said to be ill-posed. Despite the negative connotations, the study of ill-posed problems may nevertheless be interesting and relevant, as exemplified by the design optimization problems presented in Part I. We note that well-posedness, as characterized by properties (i)–(iii), depends on the chosen solution concept and on the topology that defines continuity. Although the solution to a well-posed problem depends continuously on data, the dependence can be very sensitive; that is, small, albeit finite, changes in data may lead to vastly different solutions. This sensitivity of the solution affects the expected accuracy of numerical discretizations of the problem. The *condition number* quantifies the sensitivity of the numerical solution, and discretized problems with small condition numbers are said to be well-conditioned, while those with large condition numbers are said to be ill-conditioned [60, § 12]. The somewhat arbitrary distinction between large and small condition numbers has to be determined on a case-by-case basis. It is important to note that well-posed problems may lead to ill-conditioned discrete problems, while ill-posed problems always lead to ill-conditioned discrete problems.

In 1958 Kurt Otto Friedrichs [25] introduced so-called *symmetric positive* differential operators

$$T\xi := \sum_i A_i \partial_i \xi + B\xi, \tag{8.1}$$

where ∂_i denotes partial differentiation with respect to the ith (space–time) coordinate, each A_i is a symmetric (sufficiently regular) real matrix field, and the symmetric part of the (sufficiently regular) real square matrix field $2B - \sum_i \partial_i A_i$ is positive definite, that is,

$$B + B^T - \sum_i \partial_i A_i > 0. \tag{8.2}$$

It should be noted that equations involving symmetric positive operators do not respect the conventional, although far from exhaustive, classification of partial differential equations as either *elliptic, parabolic,* or *hyperbolic*. In fact, Friedrichs' motivation was the study of type-changing equations, such as those modeling transonic

flows. We will refer to systems of partial differential equations involving symmetric positive operators (8.1) as Friedrichs systems. For the treatment of boundary value problems on a bounded (sufficiently regular) domain Q involving symmetric positive operators (8.1), Friedrichs introduced so-called semi admissible homogeneous boundary conditions

$$M\xi = 0 \quad \text{on } \partial Q, \tag{8.3}$$

where M is a (sufficiently regular) real square matrix field that satisfies a particular positivity assumption. The positivity assumptions on the operator (8.1) and on the boundary matrix (8.3) imply a so-called Friedrichs inequality; that is, there is a constant C such that, for any $\xi \in C^1(\bar{Q})$ with $M\xi = 0$ on ∂Q,

$$\|\xi\| \leq C\|T\xi\|, \tag{8.4}$$

where $\|\xi\| = \left(\int_Q |\xi|^2\right)^{1/2}$ denotes the norm on $L^2(Q)$. Note that here, initial conditions are interpreted as boundary conditions on a space–time domain. Inequality (8.4) demonstrates that *classical solutions* to semi admissible boundary value problems of the form

$$T\xi = f \quad \text{in } Q, \tag{8.5a}$$
$$M\xi = 0 \quad \text{on } \partial Q, \tag{8.5b}$$

where $f \in C(\bar{Q})$ is a given source term, are unique and depend continuously on the data. As pointed out by Friedrichs, the formal adjoint (in the $L^2(Q)$ inner product $(\xi, \psi) = \int_Q \xi^T \psi$) of the symmetric positive operator (8.1) is given by

$$\begin{aligned} \tilde{T}\xi &:= -\sum_i \partial_i \left(A_i \xi\right) + B^T \xi = -\sum_i A_i \partial_i \xi - \left(\sum_i \partial_i A_i\right) \xi + B^T \xi \\ &=: \sum_i \tilde{A}_i \partial_i \xi + \tilde{B}\xi. \end{aligned} \tag{8.6}$$

By noting that $\tilde{A}_i = \tilde{A}_i^T$ and

$$\tilde{B} + \tilde{B}^T - \sum_i \partial_i \tilde{A}_i = T + \tilde{T} = B + B^T - \sum_i \partial_i A_i, \tag{8.7}$$

we find that the formal adjoint operator $\tilde{T}$ is also symmetric positive. To the formal adjoint operator (8.6), Friedrichs associated the semi admissible homogeneous boundary condition

$$\tilde{M}\xi = 0 \quad \text{on } \partial Q. \tag{8.8}$$

Note that boundary conditions (8.8) and (8.3) are in general different. Since the formal adjoint operator (8.6) is symmetric positive and the boundary condition (8.8) is semi admissible, there is a constant C such that, for any $\xi \in C^1(\bar{Q})$ with $\tilde{M}\xi = 0$ on ∂Q,

$$\|\xi\| \leq C\|\tilde{T}\xi\|. \tag{8.9}$$

By inequality (8.9), Friedrichs deduced existence of *weak solutions* to the semi admissible boundary value problem (8.5) with data in $L^2(Q)$. That is, for any $f \in L^2(Q)$ there is $\xi \in L^2(Q)$ such that, for all $\eta \in C^1(\bar{Q})$ with $\tilde{M}\eta = 0$ on ∂Q,

$$(\tilde{T}\eta, \xi) = (\eta, f). \tag{8.10}$$

To complete the well-posedness triad (i)–(iii), it remains either to demonstrate existence of classical solutions, or uniqueness and continuous dependence on data of weak solutions, depending on the desired solution concept. If a weak solution ξ also is a *strong solution*, that is, there is a sequence $(\xi_k)_{k\in\mathbb{N}} \subset C^1(\bar{Q})$ with $M\xi_k = 0$ on ∂Q such that $\xi_k \to \xi$ and $T\xi_k \to f$ in $L^2(Q)$, the Friedrichs inequality (8.4) holds, and thereby uniqueness and continuous dependence on data. Friedrichs treated problems for which the boundary is not a characteristic surface of the differential operator $\sum_i A_i\partial_i$, that is, problems for which the boundary matrix

$$A_n \coloneqq \sum_i A_i n_i \tag{8.11}$$

is invertible. In definition (8.11), n_i denotes the ith component of the outward unit normal field to the boundary. Moreover, to demonstrate that a weak solution satisfies the boundary condition (8.3) in a strong sense, Friedrichs required the boundary conditions (8.3) and (8.8) to be *strictly adjoint* in a particular sense. Semi admissible boundary conditions (8.3) and (8.8) that are strictly adjoint are said to be admissible. There are at least three equivalent characterizations of admissible boundary conditions [1, 19]. For instance, they may be characterized by pairs of subspaces $N = \{\xi \mid M\xi = 0\}$ and $\tilde{N} = \{\xi \mid \tilde{M}\xi = 0\}$ that are defined point-wise on the boundary and satisfy the point-wise properties

$$\xi^T A_n \xi \geq 0 \text{ for all } \xi \in N \text{ and } \xi^T A_n \xi \leq 0 \text{ for all } \xi \in \tilde{N}, \tag{8.12a}$$

$$N = (A_n\tilde{N})^\perp \text{ and } \tilde{N} = (A_n N)^\perp, \tag{8.12b}$$

where $(A_n\tilde{N})^\perp = \{\xi \mid \xi^T A_n \eta = 0 \text{ for all } \eta \in \tilde{N}\}$, and analogously $(A_n N)^\perp = \{\xi \mid \xi^T A_n \eta = 0 \text{ for all } \eta \in N\}$.

The existing literature on Friedrichs systems is extensive. Here, we briefly review some contributions that are of particular relevance for this thesis.

Rauch [50] extends Friedrichs' analysis to boundaries that are characteristic with constant multiplicity; that is, the dimension of the null space of A_n is fixed on (each connected component of) the boundary. In conjunction with operator (8.1), Rauch introduces the graph space

$$W = \{\xi \in L^2(Q) \mid T\xi \in L^2(Q)\} \tag{8.13}$$

equipped with the so-called graph norm satisfying $\|\cdot\|_W^2 \coloneqq \|\cdot\|^2 + \|T\cdot\|^2$. Assuming regularity of the coefficient matrices A_i and B, the domain Q, and its boundary ∂Q, Rauch establishes density of $C^1(\bar{Q})$ in the graph space and introduces boundary traces that give precise meaning to boundary conditions of the form (8.3) and (8.8) for elements in the graph space. Rauch demonstrates that any $\xi \in W$ that satisfies $M\xi = 0$ on ∂Q can be approximated to desired accuracy in the graph norm by a function $\psi \in C^1(\bar{Q})$ that satisfies $M\psi = 0$ on ∂Q, and thus that a weak solution satisfying the boundary condition (8.3) is a strong solution. Indeed, if $\xi \in L^2(Q)$ is a weak solution, then equation (8.10) holds for all $\eta \in C_0^1(Q)$, which demonstrates that $\xi \in W$ by the definition of weak derivatives. Rauch completes the well-posedness triad by demonstrating that, for each $f \in L^2(Q)$, there is a constant C and a unique $u \in L^2(Q)$ that satisfies the equation $Tu = f$ in Q, the admissible boundary condition $Mu = 0$ on ∂Q, and the Friedrichs inequality $\|u\| \leq C\|Tu\| \equiv C\|f\|$.

The thesis of Jensen [38] provides an extensive and modern exposition of the theory of Friedrichs systems and analyzes discontinuous Galerkin finite element methods for the discretization of these. General properties of graph spaces of first order differential operators are developed; in particular, boundary trace operators on the graph spaces are constructed and analyzed in detail. Jensen presents a number of theorems addressing the well-posedness triad and remarks that the main technical difficulty in developing a theory for Friedrichs systems is the proper handling of boundary traces and boundary conditions.

Ern, Guermond, & Caplain [24] present an abstract theory for Friedrichs systems with an intrinsic characterization of admissible boundary conditions that is free from boundary traces. In the abstract theory, L is a Hilbert space, $\mathcal{D}$ is a dense subspace of L, and $T, \tilde{T} : \mathcal{D} \to L$ are linear operators that satisfy the condition

$$(T\phi, \psi)_L = (\phi, \tilde{T}\psi)_L \quad \text{for all } \phi, \psi \in \mathcal{D}, \tag{8.14}$$

and the bound

$$\|(T + \tilde{T})\phi\|_L \leq C\|\phi\|_L \quad \text{for all } \phi \in \mathcal{D} \tag{8.15}$$

for some constant C. For the classical setting of Friedrichs systems presented above, we would consider $L = L^2(Q)$ and $\mathcal{D} = C_0^1(Q)$, and condition (8.14) states that T and $\tilde{T}$ are formally adjoint. Note that condition (8.14) implies that

$$\big((T \pm \tilde{T})\phi, \psi\big)_L = \big(\phi, (\tilde{T} \pm T)\psi\big)_L \quad \text{for all } \phi, \psi \in \mathcal{D}. \tag{8.16}$$

Thus, combining property (8.16) and bound (8.15), we find that $T = \frac{1}{2}(T - \tilde{T}) + \frac{1}{2}(T + \tilde{T})$ is the sum of a "formally skew-symmetric" operator and a "formally symmetric" bounded operator. The operators T and $\tilde{T}$ extend[1] to bounded operators $L \to W_0'$, where W_0' denotes the dual space of W_0, where W_0 is the completion of $\mathcal{D}$ in the graph norm $\|\cdot\|_W = \sqrt{\|\cdot\|_L^2 + \|T\cdot\|_L^2}$. We use the same symbols for the extended operators. The graph space $W = \{\xi \in L \mid T\xi \in L\} \supset W_0$ is a Hilbert space in the graph norm. Ern, Guermond, and Caplain introduce the operator $\mathfrak{D} : W \to W'$ by the expression

$$\langle \mathfrak{D}\xi, \psi\rangle_W = (T\xi, \psi)_L - (\xi, \tilde{T}\psi)_L, \tag{8.17}$$

where $\xi, \psi \in W$, and $\langle\cdot,\cdot\rangle_W$ denotes the duality pairing on $W' \times W$. It turns out that $\ker \mathfrak{D} = W_0$, so the operator $\mathfrak{D}$ may be interpreted as an abstract boundary operator and expression (8.17) as an abstract integration-by-parts formula. Indeed, in the classical setting, $L = L^2(Q)$ and therefore

$$\int_{\partial Q} \psi^T A_n \xi = (T\xi, \psi) - (\xi, \tilde{T}\psi) \equiv \int_\Omega \psi^T T\xi - \int_Q \xi^T \tilde{T}\psi \tag{8.18}$$

for any $\xi, \psi \in C^1(\bar{Q})$. Abstract (admissible) boundary conditions are encoded in a pair of spaces $V, \tilde{V} \subset W$ that satisfy the conditions

$$\langle \mathfrak{D}\xi, \xi\rangle_W \geq 0 \text{ for all } \xi \in V \text{ and } \langle \mathfrak{D}\xi, \xi\rangle_W \leq 0 \text{ for all } \xi \in \tilde{V}, \tag{8.19a}$$

$$V = (\mathfrak{D}\tilde{V})^\perp \text{ and } \tilde{V} = (\mathfrak{D}V)^\perp, \tag{8.19b}$$

[1] The extension process is detailed, for instance, by Antonić & Burazin [1].

where $(\mathfrak{D}V)^\perp = \{\psi \in W \mid \langle \mathfrak{D}\xi, \psi\rangle_W = 0 \; \forall \xi \in V\}$, and $(\mathfrak{D}\tilde{V})^\perp = \{\psi \in W \mid \langle \mathfrak{D}\xi, \psi\rangle_W = 0 \; \forall \xi \in \tilde{V}\}$. Note the similarity of conditions (8.19) and (8.12). Ern, Guermond, and Caplain consider the following abstract problem.

$$\text{Given } f \in L, \text{ find } \xi \in V \text{ such that } T\xi = f. \tag{8.20}$$

To demonstrate well-posedness of problem (8.20), they require in addition to conditions (8.14), (8.15), and (8.19) that there is a positive constant C such that

$$\big((T + \tilde{T})\phi, \phi\big)_L \geq C\|\phi\|_L^2 \quad \text{for any } \phi \in \mathcal{D}. \tag{8.21}$$

Note that identity (8.7) reveals that condition (8.21) corresponds to positivity (8.2) in the classical setting.

Both the classical and abstract theories of Friedrichs systems above lead to space-time formulations of initial–boundary value problems. Recently, Burazin & Erceg [20] presented a theory for abstract initial–boundary value problems based on semigroup theory. More precisely, they prove that the unbounded operator $-T|_V : V \subset L \to L$ is the generator of a strongly continuous semigroup of contractions $(S(t))_{t\geq 0}$ on L. If, for some $\tau > 0$, $f \in C^1([0,\tau], L)$ and $\xi_{\mathrm{I}} \in V$, then $\xi \in C([0,\tau], L) \cap C^1((0,\tau), V)$ defined by

$$\xi(t) = S(t)\xi_{\mathrm{I}} + \int_0^t S(t-s)f(s)\,\mathrm{d}s \tag{8.22}$$

is the unique solution to the abstract initial(–boundary) value problem [47, § 4.2 Cor. 2.5]

$$\partial_t \xi(t) = -T\xi(t) + f \quad t \in (0,\tau), \tag{8.23a}$$

$$\xi(0) = \xi_{\mathrm{I}}. \tag{8.23b}$$

Moreover, recalling that $(S(t))_{t\geq 0}$ in expression (8.22) is a family of contractions, we find that

$$\sup_{t\in[0,\tau]} \|\xi(t)\|_L \leq \|\xi_{\mathrm{I}}\|_L + \int_0^\tau \|f(s)\|_L\,\mathrm{d}s, \tag{8.24}$$

which completes the well-posedness triad for problem (8.23). Bounds of the form (8.24) are often referred to as energy estimates. Note that for $f \in L^1((0,\tau), L)$ and $\xi_{\mathrm{I}} \in L$, formula (8.22) defines $\xi \in C([0,\tau], L)$ as the unique mild solution [47, § 4.2 Def. 2.3] to problem (8.23) satisfying bound (8.24). Therefore, problem (8.23) is mildly well-posed.

Ern, Guermond, and Caplain's proof of well-posedness of problem (8.20), relies on the following characterization, attributed to Nečas [46]. The problem (8.20) is well-posed if and only if

(i) there is an $\alpha > 0$ such that, for each $\xi \in V$, $\sup\limits_{\substack{\psi\in L\\ \psi\neq 0}} \dfrac{(\psi, T\xi)_L}{\|\psi\|_L} \geq \alpha\|\xi\|_V$, and

(ii) if $\psi \in L$ satisfies $(\psi, T\xi)_L = 0$ for each $\xi \in V$, then $\psi = 0$.

We see that Nečas' characterization of well-posedness is centered on the bounded bilinear form $a : L \times V \to \mathbb{R}$ defined by $a(\psi, \xi) = (\psi, T\xi)_L$. In fact, the abstract problem (8.20) is equivalent to the following variational problem.

$$\text{Given } f \in L, \text{ find } \xi \in V \text{ such that } a(\psi, \xi) = l(\psi) \text{ for all } \psi \in L, \tag{8.25}$$

where the bounded linear form $l : L \to \mathbb{R}$ is defined by $l(\psi) = (\psi, f)_L$. Note that problem (8.25) displays the generic form of *variational formulations* in which the forms a and b are defined on a pair of linear spaces V and L. In the context of variational formulations, V is called the trial space and L the test space.

Variational formulations are at the heart of finite element methods, which are routinely applied to generate numerical approximations to initial–boundary value problems. In particular, specialized discontinuous Galerkin methods have been developed for discretizing Friedrichs systems, for instance, by Jensen [38]. Nonetheless, it appears that variational formulations of Friedrichs systems are rarely analyzed in the scientific literature. A notable exception is the variational least-squares treatment by Azerad [2] of the linear transport equation

$$\partial_t \xi + \beta \cdot \nabla \xi = f, \tag{8.26}$$

where β is a given vector field, and f a source. We note that least-squares formulations, in which a quadratic residual is minimized, is a general source for variational formulations, as described, for instance, by Bochev & Gunzburger [7]. In the particular case of transport equation (8.26), Azerad's least-squares formulation corresponds to an equivalent second-order anisotropic diffusion problem that accordingly leads to a variational formulation in which both the trial and test spaces are *contained* in the graph space of the operator. This is in contrast to variational formulation (8.25) as well as to the variational formulations developed in Publication V for which the test space *contains* the graph space.

The particular variational formulation (8.25) and the other formulations given above treat homogeneous boundary conditions that are included in the definitions of the function spaces, such as, V and $\tilde{V}$; thus, inhomogeneous boundary conditions need to be lifted to the interior and incorporated in the source term f. Although theoretically convenient, the lifting of an inhomogeneous boundary condition in practice requires solving a boundary value problem, which may be of similar complexity as the original problem. Moreover, boundary conditions that are included in the definition of the spaces often require special treatment in numerical solution procedures. The variational formulations developed in Publication V are constructed to treat inhomogeneous initial–boundary value problems without the need for lifting. In Publication V, we assume that the source, the initial data, and the boundary data belong to suitable L^2 spaces. Accordingly, the trial space is defined as a subspace of the graph space that admits L^2 boundary[2] traces, and the trial space is chosen as a tuple of L^2 spaces, which are used to independently enforce the equations, the initial conditions, and the boundary conditions.

In the next chapter, we present Friedrichs systems that model linear acoustics, for instance the propagation of sound in air. These provide a selection of the Friedrichs systems studied in Publications V and VI.

[2] Recall that initial conditions may be regarded as boundary conditions on a space-time domain.

9. Linear acoustics

Linear acoustics is the study of small amplitude fluctuations of a medium. In this thesis, we limit the discussion to fluid media whose motions are well-modeled by Euler's equations under isentropic conditions,

$$\rho Du + \nabla p = \rho\varphi, \tag{9.1a}$$
$$D\rho + \rho\nabla \cdot u = 0, \tag{9.1b}$$
$$Ds = 0, \tag{9.1c}$$
$$p = \Sigma(\rho, s), \tag{9.1d}$$

where u, p, ρ, s, and φ denote the flow velocity, pressure, density, (specific) entropy, and volume force density fields, respectively, and $D = \partial_t + u \cdot \nabla$ the material derivative. The equations (9.1a)–(9.1c) express conservation of momentum, mass, and energy, respectively, and the equation of state (9.1d), which is of thermodynamic origin, provides closure of the system. We assume that the domain is a sufficiently regular space-time cylinder $Q = \Omega \times (0, \tau) \subset \mathbb{R}^d \times \mathbb{R}$.

9.1 Linearized Euler's equations

Introducing the linearization ansatz

$$u(x,t) = u_0(x,t) + \delta u(x,t), \tag{9.2}$$

where u_0 is a given background flow velocity field and δu the so-called Eulerian perturbation of u, and analogous ansatzes for the other fields into Euler's equations (9.1), expanding and equating terms of like powers in the perturbations, we find to zeroth order

$$\rho_0 D_0 u_0 + \nabla p_0 = \rho_0 \varphi_0, \tag{9.3a}$$
$$D_0\rho_0 + \rho_0\nabla \cdot u_0 = 0, \tag{9.3b}$$
$$D_0 s_0 = 0, \tag{9.3c}$$
$$p_0 = \Sigma(\rho_0, s_0), \tag{9.3d}$$

and to first order

$$\rho_0 D_0\,\delta u + \nabla\delta p + \rho_0(\delta u \cdot \nabla)u_0 - \frac{\nabla p_0}{\rho_0}\delta\rho = \rho_0\,\delta\varphi, \tag{9.4a}$$
$$D_0\,\delta\rho + \rho_0\nabla \cdot \delta u + (\delta u \cdot \nabla)\rho_0 + (\nabla \cdot u_0)\delta\rho = 0, \tag{9.4b}$$
$$D_0\,\delta s + (\delta u \cdot \nabla)s_0 = 0, \tag{9.4c}$$
$$\delta p = c_0^2\,\delta\rho + \alpha_0\,\delta s, \tag{9.4d}$$

where $D_0 = \partial_t + u_0 \cdot \nabla$ denotes the material derivative with respect to the background flow velocity u_0, $c_0^2 = \Sigma_{,1}(\rho_0, s_0)$[1] the squared speed of sound, and $\alpha_0 =$

[1] $\Sigma_{,i}$ denotes the derivative of Σ with respect to the ith argument.

$\Sigma_{,2}(\rho_0, s_0)$. Thus, the background flow is also a solution to Euler's equations (9.3), and the perturbations satisfy the linearized Euler's equations (9.4) to first order. Note that it is assumed that the density and speed of sound are uniformly positive; that is, there are constants $\underline{\rho_0}, \underline{c_0}$ such that

$$\rho_0 \geq \underline{\rho_0} > 0 \text{ and } c_0 \geq \underline{c_0} > 0 \text{ in } \bar{Q}. \tag{9.5}$$

For particular combinations of equations of state and background flows, the linearized Euler's equations are simplified and may even be reduced to a scalar wave equation. For instance, if the medium is an ideal gas, the background flow is steady, stagnant ($u_0 = 0$), and subject to a negligible volume force density ($\phi_0 = 0$), then

$$\partial_t(\rho_0 c_0\, \delta u) + c_0 \nabla \delta p = \rho_0 c_0\, \delta\varphi, \tag{9.6a}$$

$$\partial_t \delta p + \nabla \cdot \big(c_0(\rho_0 c_0\, \delta u)\big) = 0, \tag{9.6b}$$

from which follows that the Eulerian pressure perturbation δp satisfies the inhomogeneous wave equation (compare with the derivation by Rienstra & Hirschberg [51, § 2.4])

$$\partial_t^2 \delta p - \nabla \cdot (c_0^2 \nabla \delta p) = -\rho_0 c_0^2 \nabla \cdot \delta\varphi. \tag{9.7}$$

If δp is a solution to wave equation (9.7), then the corresponding velocity perturbation δu is given by the following formula, which is deduced from equation (9.6a).

$$\delta u(x,t) = \delta u_{\mathrm{I}}(x) + \int_0^t \left(\delta\varphi(x,t') - \frac{\nabla \delta p(x,t')}{\rho_0(x)}\right) \mathrm{d}t', \tag{9.8}$$

where δu_{I} denotes the initial velocity perturbation that satisfies

$$(\partial_t \delta p)|_{t=0} = -\nabla \cdot (\rho_0 c_0^2\, \delta u_{\mathrm{I}}). \tag{9.9}$$

Note that equation (9.9), which is inferred from equation (9.6b), can be interpreted as the initial condition on $\partial_t \delta p$. Similarly, equations (9.4c) and (9.4d), yield formulæ

$$\delta s(x,t) = \delta s_{\mathrm{I}}(x) - \int_0^t \big(\delta u(x,t') \cdot \nabla\big) s_0(x)\, \mathrm{d}t', \tag{9.10a}$$

$$\delta\rho(x,t) = \frac{\delta p(x,t) - \alpha_0(x)\, \delta s(x,t)}{c_0(x)^2}, \tag{9.10b}$$

where δs_{I} denotes the initial entropy perturbation.

To connect to the presentation of Friedrichs systems in Chapter 8, we note that system (9.6) is expressible as

$$T\xi \coloneqq \begin{pmatrix} \partial_t & c_0 \nabla \\ \nabla \cdot (c_0\ \ ) & \partial_t \end{pmatrix} \begin{pmatrix} \rho_0 c_0\, \delta u \\ \delta p \end{pmatrix} = \begin{pmatrix} \rho_0 c_0\, \delta\varphi \\ 0 \end{pmatrix} =: f. \tag{9.11}$$

We note that $\tilde{T} = -T$ is the formal adjoint of T in the regular $L^2(Q)$ inner product, so $T + \tilde{T} = 0$ is bounded but not positive. However, let us identify the formal adjoint of T in the weighted $L^2(Q)$ inner product $(\psi, \xi)_\mu = \int_Q \mu\, \psi^T \xi$, where

$$\mu(x,t) = \exp(-\lambda t) \tag{9.12}$$

for some $\lambda > 0$. Integrating by parts, we find

$$(T\xi, \psi)_\mu = (\xi, -T\psi + \lambda\psi)_\mu =: (\xi, \tilde{T}\psi)_\mu \text{ for any } \psi, \xi \in C_0^1(Q), \tag{9.13}$$

so $T + \tilde{T} = \lambda I$ is bounded and positive, and therefore problem (9.11) is of Friedrichs type. Another trick to incorporate the problem into the class of Friedrichs systems is to note that, for any $\lambda > 0$, problem (9.11) is equivalent to

$$\mu T\xi = \mu f; \tag{9.14}$$

and the formal adjoint in the regular $L^2(Q)$ inner product of $T_\mu := \mu T$ is $\tilde{T}_\mu := \lambda\mu - T_\mu$, so $T_\mu + \tilde{T}_\mu = \lambda\mu I$ is bounded and positive. Yet another trick, which was employed already by Friedrichs [25], is to consider $\xi_\mu := \mu\xi$ as a new unknown in problem (9.14), and noting that $\mu T\xi = \mu T((1/\mu)\mu\xi) = \lambda\xi_\mu + T\xi_\mu$. Thus, problem (9.11) is equivalent to

$$T\xi_\mu + \lambda\xi_\mu = \mu f, \tag{9.15}$$

and $\tilde{T}_\lambda := -T + \lambda I$ is the formal adjoint of $T_\lambda := T + \lambda I$ in the regular $L^2(Q)$ inner product, so $\tilde{T}_\lambda + T_\lambda = 2\lambda I$ is bounded and positive.

In the third example of Publication V, we develop a well-posed variational formulation of an inhomogeneous initial–boundary value problem for system (9.6).

Publication VI treats the case of barotropic flows. Barotropic conditions hold for elastic fluids, for which pressure is a function of density only, or when the conditions are homentropic, that is, $s = s_0$ is uniform and constant. Then, in particular, $\alpha_0\,\delta s = 0$, so the linearized equation of state (9.4d) reduces to

$$\delta p = c_0^2\,\delta\rho. \tag{9.16}$$

With the aid of relation (9.16), equations (9.4a) and (9.4b) are expressible as a system in δu and δp, or δu and $\delta\rho$. However, choosing the variables δu and $\delta\hat{\rho} := c_0\delta\rho/\rho_0$ $(= \delta p/(\rho_0 c_0) =: \delta\hat{p})$ as suggested by Kreiss & Lorenz [40, § 8.3], we instead obtain the system

$$T\xi := \left(\begin{pmatrix} \rho_0 D_0 & \nabla(\rho_0 c_0\,) \\ \rho_0 c_0 \nabla\cdot & \rho_0 D_0 \end{pmatrix} + \rho_0 c_0 \begin{pmatrix} \dfrac{\nabla u_0}{c_0} & -\dfrac{\nabla\rho_0}{\rho_0} \\ \dfrac{\nabla\rho_0}{\rho_0}\cdot & -\dfrac{D_0 c_0}{c_0^2} \end{pmatrix} \right) \begin{pmatrix} \delta u \\ \delta\hat{\rho} \end{pmatrix} = \begin{pmatrix} \rho_0\delta\varphi \\ 0 \end{pmatrix} =: f. \tag{9.17}$$

Note, to arrive at formulation (9.17), we used that for barotropic flows the equation of state (9.3d) implies that $\nabla p_0 = c_0^2\nabla\rho_0$. Mass conservation (9.3b) implies that, for sufficiently smooth scalar fields ϕ, ψ,

$$\begin{aligned} \partial_t(\rho_0\,\psi\phi) + \nabla\cdot(\rho_0 u_0\,\psi\phi) &= \psi\phi\,(\underbrace{\partial_t\rho_0 + \nabla\cdot(\rho_0 u_0)}_{=0}) + \rho_0\partial_t(\psi\phi) + (\rho_0 u_0\cdot\nabla)(\psi\phi) \\ &= \rho_0 D_0(\psi\phi) = \psi\,\rho_0 D_0\phi + \phi\,\rho_0 D_0\psi. \end{aligned} \tag{9.18}$$

With the aid of identity (9.18) and the divergence theorem, we find that

$$\tilde{T} := -\begin{pmatrix} \rho_0 D_0 & \nabla(\rho_0 c_0\,) \\ \rho_0 c_0 \nabla\cdot & \rho_0 D_0 \end{pmatrix} + \rho_0 c_0 \begin{pmatrix} \dfrac{(\nabla u_0)^T}{c_0} & \dfrac{\nabla\rho_0}{\rho_0} \\ -\dfrac{\nabla\rho_0}{\rho_0}\cdot & -\dfrac{D_0 c_0}{c_0^2} \end{pmatrix} \tag{9.19}$$

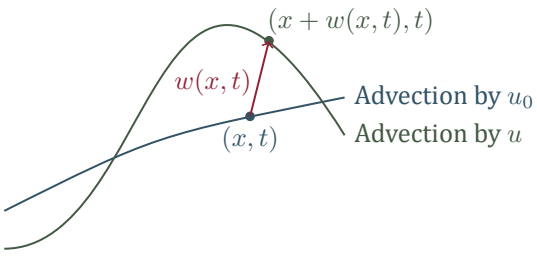

Figure 9: The Lagrangian displacement w.

is the formal adjoint of T in $L^2(Q)$. For sufficiently regular background flows, $T + \tilde{T}$ is bounded, but not positive in general. Nevertheless, the same weighting tricks that resolved the positivity issue for system (9.11) also work here.

In Publication VI, we develop a mildly well-posed formulation of an initial–boundary value problem for the barotropic system (9.17). This system is of importance in, for instance, aeroacoustics where it serves as a model of lossless propagation of acoustic disturbances in the presence of a background flow.

9.2 The Lagrangian displacement and Galbrun's equation

Traditionally, the Lagrangian displacement vector field w is defined as the displacement of individual fluid particles, as illustrated in Figure 9 and detailed in Appendix A of Publication VI. In particular, it follows that, to first order in w and δu, the Lagrangian displacement satisfies

$$\delta u = D_0 w - (w \cdot \nabla) u_0 \equiv (\partial_t + \mathcal{L}_{u_0})\, w, \tag{9.20}$$

where $\mathcal{L}_{u_0} w = (u_0 \cdot \nabla) w - (w \cdot \nabla) u_0 = -\mathcal{L}_w u_0$ denotes the Lie derivative of w with respect to u_0. Thus, the velocity perturbation is computable from the Lagrangian displacement.

In 1931, Henri Galbrun [27, § 3] appears to have been the first of many to develop a linear second order partial differential equation for the evolution of the Lagrangian displacement. The following formulation of Galbrun's equation is an adaptation to our notation of the formulation derived by Gabard [26] in his dissertation.

$$\rho_0 D_0^2 w - \nabla(\rho_0 c_0^2 \nabla \cdot w) + (\nabla p_0) \nabla \cdot w - (\nabla w)^T \nabla p_0 - \rho_0 (w \cdot \nabla) \varphi_0 = \rho_0\, \delta\varphi. \tag{9.21}$$

One advantage of formulation (9.21) is that in frequency domain it naturally leads to a variational formulation that contains no derivatives of the background flow quantities other than ∇p_0 [12]. We have already seen that the velocity perturbation is

computable from the Lagrangian displacement by formula (9.20). The derivation of Galbrun's equation (9.21), requires that the remaining perturbations satisfy

$$\delta\rho = -\nabla \cdot (\rho_0 w), \tag{9.22a}$$

$$\delta s = -(w \cdot \nabla) s_0, \tag{9.22b}$$

$$\delta p = -\rho_0 c_0^2 \nabla \cdot w - (w \cdot \nabla) p_0 \equiv c_0^2 \, \delta\rho + \alpha_0 \, \delta s, \tag{9.22c}$$

where the last identity follows from $\nabla p_0 = c_0^2 \nabla \rho_0 + \alpha_0 \nabla s_0$, which is a consequence of state equation (9.4d). A tedious calculation demonstrates that if the Lagrangian displacement satisfies Galbrun's equation (9.21), then the perturbations given by formulæ (9.20) and (9.22) satisfy the linearized Euler's equations (9.4). The conclusion is that *all perturbations are computable from the Lagrangian displacement*.

The derivation of Galbrun's equation presented in Gabard's dissertation [26] employs a so-called Lagrangian linearization ansatz to Euler's equations (9.1). The Lagrangian linearization ansatz involves Lagrangian perturbations

$$\delta_L u(x,t) = \delta u(x,t) + (w(x,t) \cdot \nabla) \, u_0(x,t) \approx u(x + w(x,t), t) - u_0(x,t), \tag{9.23}$$

and analogous expressions for the other fields. Brazier [17] presents a derivation of Galbrun's equation, attributed to Poirée [49], in which Euler's equations are expressed and linearized in a Lagrangian (material) frame of reference before returning to the Eulerian (fixed) frame of reference. Godin [29] develops Galbrun's equation for an oscillatory displacement field and demonstrates that the oscillatory displacement is equal to the Lagrangian displacement to first order. In Publication VI, we present a derivation of Galbrun's equation for barotropic background flows that does not rely on Lagrangian perturbations and in which the Lagrangian displacement is abstractly introduced as a solution to equation (9.20).

To the best of our knowledge, all derivations of Galbrun's equation rely, explicitly or implicitly, on the so-called *"no resonance" assumption* that was formalized by Godin [29]:

> *Let h depend linearly on some combination of $\delta u, \delta\rho, \delta p, \delta s, w$, and their derivatives. If $D_0 h = 0$, then $h \equiv 0$.*

Indeed, by introducing formula (9.20) into equation (9.4b), we demonstrate in Publication VI that

$$D_0 \left(\frac{\delta\rho + \nabla \cdot (\rho_0 w)}{\rho_0} \right) = 0. \tag{9.24}$$

Similarly, by formula (9.20), we obtain the identity $\delta u \cdot \nabla s_0 = D_0(w \cdot \nabla s_0) + (w \cdot \nabla) D_0 s_0$, which together with equations (9.3c) and (9.4c) demonstrates that

$$D_0 \left(\delta s + w \cdot \nabla s_0 \right) = 0. \tag{9.25}$$

The required formulas (9.22a) and (9.22b) then follow from the "no resonance" assumption. The term "no resonance" derives from the fact that $h(x,t) = \exp(i\omega t - ik \cdot x)$ is a non-trivial solution to $D_0 h = 0$ for uniform u_0, provided that $\omega = k \cdot u_0$, that is, provided ω and k are 'in resonance' with u_0. In Publication VI, we exploit that on a bounded domain $Q = \Omega \times (0, \tau)$, for a sufficiently regular background flow and quantity h, the "no resonance" assumption is fulfilled if and only if h vanishes initially and on the space-time boundary part where the background flow is entering.

On the one hand, if the "no resonance" assumption holds, and h is a scalar field that is sufficiently regular to admit boundary traces on ∂Q, then $h = 0$ in Q implies that $h = 0$ on ∂Q. On the other hand, assume that h is a sufficiently regular scalar field that satisfies $D_0 h = 0$ in Q for some sufficiently regular background flow. The space-time boundary ∂Q of the space-time cylinder $Q = \Omega \times (0, \tau)$ is naturally partitioned as $\partial Q = \overline{Q_0} \cup \overline{Q_\tau} \cup \overline{\Sigma}$, where $Q_0 \coloneqq \Omega \times \{0\}$, $Q_\tau \coloneqq \Omega \times \{\tau\}$, and $\Sigma \coloneqq \partial\Omega \times (0, \tau)$. We further partition $\Sigma = \Sigma_0 \cup \Sigma_- \cup \Sigma_+$ into parts where the background flow is tangential, entering or exiting, respectively. That is,

$$\begin{aligned} \Sigma_0 &\coloneqq \{(x,t) \in \Sigma \mid n(x) \cdot u_0(x,t) = 0\}, \\ \Sigma_- &\coloneqq \{(x,t) \in \Sigma \mid n(x) \cdot u_0(x,t) < 0\}, \\ \Sigma_+ &\coloneqq \{(x,t) \in \Sigma \mid n(x) \cdot u_0(x,t) > 0\}, \end{aligned} \tag{9.26}$$

where n denotes the outward unit normal field to $\partial\Omega$. To prove the claim, we exploit identity (9.18) with $\phi = h$ and $\psi = -\mu h$, where $\mu(x,t) = \exp(-\lambda t)$ for some $\lambda > 0$. Note that, since $D_0 h = 0$ and $D_0 \mu = -\lambda\mu$, we have that the right hand side of identity (9.18) with $\phi = h$ and $\psi = -\mu h$ equals $\lambda \rho_0 \, \mu h^2$. Thus, integrating identity (9.18) with $\phi = h$ and $\psi = -\mu h$ over the domain Q, employing the divergence theorem and properties (9.26), we obtain the bound

$$\begin{aligned} \lambda \int_Q \rho_0 \, \mu h^2 &= -\int_Q \left[\partial_t\big(\rho_0 \, \mu h^2\big) + \nabla \cdot \big(\rho_0 u_0 \, \mu h^2\big)\right] \\ &= \int_{Q_0} \rho_0 \, \mu h^2 + \int_{\Sigma_-} \rho_0 |n \cdot u_0| \, \mu h^2 - \int_{Q_\tau} \rho_0 \, \mu h^2 - \int_{\Sigma_+} \rho_0 |n \cdot u_0| \, \mu h^2 \\ &\leq \int_{Q_0} \rho_0 \, \mu h^2 + \int_{\Sigma_-} \rho_0 |n \cdot u_0| \, \mu h^2, \end{aligned} \tag{9.27}$$

which demonstrates that if $D_0 h = 0$ in Q and h vanishes on Q_0 and Σ_-, then h vanishes in Q.

In a uniform background flow, Galbrun's equation (9.21) reduces to a convected vector wave equation,

$$D_0^2 w - c_0^2 \nabla(\nabla \cdot w) = \delta\varphi. \tag{9.28}$$

Berriri et al. [5, 6] propose a regularized formulation of equation (9.28),

$$D_0^2 w - c_0^2 \nabla(\nabla \cdot w) + c_0^2 \nabla \times (\nabla \times w - \psi) = \delta\varphi, \tag{9.29}$$

where ψ satisfies

$$D_0^2 \psi = \nabla \times \delta\varphi. \tag{9.30}$$

Equation (9.30) is derived by applying the curl operator to equation (9.28) and in the end replacing $\nabla \times w$ with ψ. Note that if $\psi = \nabla \times w$, then equation (9.29) reduces to the original convected wave equation (9.28). Equations (9.30) and (9.29) may be solved in sequence, and in some cases there are even analytical expressions for ψ [5]. Berriri et al. [5, 6] develop well-posed regularized initial–boundary value problems for subsonic ($|u_0| < c_0$) background flows on an infinite 2D duct with rigid walls. Appealing to the identity

$$-\Delta w = -\nabla(\nabla \cdot w) + \nabla \times (\nabla \times w), \tag{9.31}$$

the regularized formulation avoids the need of a tailored functional setting for the spatial operator $(u_0 \cdot \nabla)^2 - c_0^2 \nabla(\nabla \cdot\ )$, which for $u_0 \neq 0$ is neither positive semi-definite nor negative semi-definite but indefinite. To reconcile the regularized formulation (9.29) with the original formulation (9.28), the initial–boundary value problems considered by Berriri et al. [5, 6] include the additional boundary condition $\nabla \times w = \psi$ on Σ. A stable scheme for discretizing the regularized formulation is devised based on Lagrange finite elements for the spatial part and finite differences for the temporal part of the operator. Due to the lack of H^1-coerciveness, the proposed scheme is found to be unstable when applied to the original convective vector wave equation (9.28).

We note that regularized formulations of Galbrun's equation (9.21) may be analogously defined for general background flows. However, the resulting pair of equations generalizing equations (9.29) and (9.30) are then fully coupled. In fact, inspired by a similar approach to Maxwell's equations, the regularized formulation was first introduced to study time-harmonic solutions to the convected vector wave equation (9.28), that is, Galbrun's equation in a uniform background flow. Well-posed boundary-value problems for regularized time-harmonic Galbrun's equation have been developed in the literature for a sequence of increasingly complicated two-dimensional subsonic background flows [8, 9, 10, 11, 12]. Also in the time-harmonic setting, naive discretizations of Galbrun's equation (9.21) are known to be poorly performing [43, 61].

In Publication VI, we analyze Galbrun's equation for barotropic background flows that are tangential to the boundary ($\Sigma = \Sigma_0$). Formally, we construct solutions to Galbrun's equation from solutions to linearized Euler's equations (9.17) by defining the Lagrangian displacement as a solution to an initial value problem for equation (9.20), where the initial datum has been tuned so that the "no resonance" assumption holds. Unfortunately, the general case of background flows that are not tangential to the boundary is not straightforward to analyze. First, the analysis of linearized Euler's equations is complicated by the fact that the boundary no longer is a characteristic surface of constant multiplicity. Second, it appears that the boundary condition on the part of the boundary where the background flow is entering the domain, which is needed to make the Lagrangian displacement well-defined, cannot be tuned to guarantee that the "no resonance" assumption holds.

10. Summary of publications: Part II

In **Publication V**, we develop well-posed variational formulations of inhomogeneous initial–boundary value problems of Friedrichs' type. In these formulations, the trial spaces are subspaces of the graph spaces that admit L^2 boundary traces, while the test spaces are tuples of L^2 spaces used to enforce the equations in the interior of the domain, the initial conditions, and the boundary conditions, respectively. The first example considered is the scalar advection–reaction equation

$$\beta \cdot \nabla u + \alpha u = f, \tag{10.1}$$

where the scalar field α is essentially bounded and uniformly positive, and the vector field β and its gradient are essentially bounded. The second example

$$u + \nabla p = f_1, \tag{10.2a}$$
$$p + \nabla \cdot u = f_2, \tag{10.2b}$$

is a first order formulation of the second order diffusion–reaction equation

$$-\Delta p + p = -\nabla \cdot f_1 + f_2. \tag{10.3}$$

The third example is the acoustical system (9.6) modeling the sound propagation in ideal stagnant media. To establish well-posedness in the form of Nečas characterization, we rely on, among other things, density in the trial spaces of functions that are smooth on the closure of the (space-time) domain.

In **Publication VI**, we analyze Galbrun's equation for barotropic background flows in bounded domains. Formally, we derive an equivalent formulation of Galbrun's equation from linearized Euler's equations (9.4) by introducing the Lagrangian displacement via equation (9.20) and invoking the "no resonance" assumption. For steady background flows that are tangential to the boundary of the domain, we develop a mildly well-posed initial–boundary value problem for linearized Euler's equations (9.17) and demonstrate that the initial condition, which is needed to make the Lagrangian displacement well-defined, may be tuned so that the "no resonance" assumption holds. We demonstrate that sufficiently regular solutions to an initial–boundary value problem for Galbrun's equation satisfy an energy estimate, even for unsteady tangential background flows. However, the possibly non-positive nature of the zeroth order terms in equations (9.17) and (9.20) prevents us from excluding the possibility that solutions grow exponentially with time.

Bibliography

[1] N. Antonić and K. Burazin. Intrinsic boundary conditions for Friedrichs systems. *Communications in Partial Differential Equations*, 35(9):1690–1715, 2010.

[2] P. Azerad. *Analyse des Équations de Navier-Stokes en Bassin peu Profond et de l'Équation de Transport.* PhD thesis, University of Neuchâtel, 1996.

[3] M. P. Bendsøe and N. Kikuchi. Generating optimal topologies in structural design using a homogenization method. *Computer Methods in Applied Mechanics and Engineering*, 71(2):197–224, 1988.

[4] M. P. Bendsøe and O. Sigmund. *Topology Optimization. Theory, Methods, and Applications*. Springer, 2003.

[5] K. Berriri. *Approche analytique et numérique pour l'aéroacoustique en régime transitoire par le modèle de Galbrun*. PhD thesis, ENSTA ParisTech, 2006.

[6] K. Berriri, A.-S. Bonnet-Ben Dhia, and P. Joly. Numerical analysis of time-dependent Galbrun equation in an infinite duct. *arXiv preprint math/0603546*, 2006.

[7] P. B. Bochev and M. D. Gunzburger. *Least-squares finite element methods*, volume 166. Springer Science & Business Media, 2009.

[8] A.-S. Bonnet-Ben Dhia, E.-M. Duclairoir, G. Legendre, and J.-F. Mercier. Time-harmonic acoustic propagation in the presence of a shear flow. *Journal of Computational and Applied Mathematics*, 204(2):428–439, 2007.

[9] A.-S. Bonnet-Ben Dhia, G. Legendre, and É. Lunéville. Analyse mathématique de l'équation de Galbrun en écoulement uniforme. *Comptes Rendus de l'Académie des Sciences-Series IIB-Mechanics*, 329(8):601–606, 2001.

[10] A.-S. Bonnet-Ben Dhia, G. Legendre, and É. Lunéville. Regularization of the time-harmonic Galbrun's equations. In *Mathematical and Numerical Aspects of Wave Propagation WAVES 2003*, pages 78–83. Springer, 2003.

[11] A.-S. Bonnet-Ben Dhia, J.-F. Mercier, F. Millot, and S. Pernet. A low-mach number model for time-harmonic acoustics in arbitrary flows. *Journal of Computational and Applied Mathematics*, 234(6):1868–1875, 2010.

[12] A.-S. Bonnet-Ben Dhia, J.-F. Mercier, F. Millot, S. Pernet, and E. Peynaud. Time-harmonic acoustic scattering in a complex flow: a full coupling between acoustics and hydrodynamics. *Communications in Computational Physics*, 11(2):555–572, 2012.

[13] T. Borrvall. *Computational Topology Optimization of Elastic Continua by Design Restriction*. Licentiate thesis, Linköping University, 2000.

[14] T. Borrvall. Topology optimization of elastic continua using restriction. *Archives of Computational Methods in Engineering*, 8(4):351–385, 2001.

[15] T. Borrvall and J. Petersson. Topology optimization using regularized intermediate density control. *Computer Methods in Applied Mechanics and Engineering*, 190(37-38):4911–4928, 2001.

[16] B. Bourdin. Filters in topology optimization. *International Journal for Numerical Methods in Engineering*, 50:2143–2158, 2001.

[17] J.-Ph. Brazier. Derivation of an exact energy balance for Galbrun equation in linear acoustics. *Journal of Sound and Vibration*, 330(12):2848–2868, 2011.

[18] T. E. Bruns and D. A. Tortorelli. Topology optimization of non-linear elastic structures and compliant mechanisms. *Computer Methods in Applied Mechanics and Engineering*, 190:3443–3459, 2001.

[19] K. Burazin. *Prilozi teoriji Friedrichsovih i hiperboličkih sustava (Contribution to the theory of Friedrichs' and hyperbolic systems)*. PhD thesis, University of Zagreb, 2008.

[20] K. Burazin and M. Erceg. Non-stationary abstract Friedrichs systems. *Mediterranean journal of mathematics*, 13(6):3777–3796, 2016.

[21] P. W. Christensen and A. Klarbring. *An introduction to structural optimization*, volume 153. Springer Science & Business Media, 2008.

[22] P. G. Ciarlet. *Linear and nonlinear functional analysis with applications*. SIAM, 2013.

[23] J. D. Deaton and R. V. Grandhi. A survey of structural and multidisciplinary continuum topology optimization: post 2000. *Structural and Multidisciplinary Optimization*, 49(1):1–38, 2014.

[24] A. Ern, J.-L. Guermond, and G. Caplain. An intrinsic criterion for the bijectivity of Hilbert operators related to Friedrich' systems. *Communications in Partial Differential Equations*, 32(2):317–341, 2007.

[25] K. O. Friedrichs. Symmetric positive linear differential equations. *Communications on Pure and Applied Mathematics*, XI:338–418, 1958.

[26] G. Gabard. *Méthodes numériques et modèles de sources aéroacoustiques fondés sur l'équation de Galbrun*. PhD thesis, Université de Technologie de Compiegne, 2003.

[27] H. Galbrun. *Propagation d'une onde sonore dans l'atmosphère et théorie des zones de silence*. Gauthier-Villars, Paris, 1931.

[28] C. A. Glasbey and R. Jones. Fast computation of moving average and related filters in octagonal windows. *Pattern Recognition Letters*, 18(6):555–565, 1997.

[29] O. A. Godin. Reciprocity and energy theorems for waves in a compressible inhomogeneous moving fluid. *Wave Motion*, 25(2):143 – 167, 1997.

[30] J. K. Guest. Topology optimization with multiple phase projection. *Computer Methods in Applied Mechanics and Engineering*, 199(1–4):123–135, 2009.

[31] J. K. Guest, J. H. Prévost, and T. Belytschko. Achieving minimum length scale in topology optimization using nodal design variables and projection functions. *International Journal for Numerical Methods in Engineering*, 61(2):238–254, 2004.

[32] M. E. Gurtin. *An introduction to continuum mechanics*. Academic Press, 2003.

[33] E. Hassan. *Topology optimization of antennas and waveguide transitions*. PhD thesis, Umeå University, Sweden, 2015.

[34] E. Hassan, D. Noreland, E. Wadbro, and M. Berggren. Topology optimisation of wideband coaxial-to-waveguide transitions. *Scientific Reports*, 7:45110, 2017.

[35] E. Hassan, E. Wadbro, and M. Berggren. Topology optimization of metallic antennas. *IEEE Transactions on Antennas and Propagation*, 63(5):2488–2500, 2014.

[36] H. J. A. M. Heijmans. Mathematical morphology: A modern approach in image processing based on algebra and geometry. *SIAM Review*, 37(1):1–36, 1995.

[37] J. D. Jackson. *Classical electrodynamics*. Wiley, New York, 3. ed. edition, 1999.

[38] M. Jensen. *Discontinuous Galerkin Methods for Friedrichs Systems with Irregular Solutions*. PhD thesis, University of Oxford, 2004.

[39] A. N. Kolmogorov. On the notion of mean. In A. N. Kolmogorov and V. M. Tikhomirov, editors, *Selected works of A.N. Kolmogorov. Vol. 1, Mathematics and mechanics*, pages 144–146. Kluwer, 1991. (Translation of: Kolmogorov A.N.: Sur la notion de la moyenne. Atti Accad. Naz. Lincei **12**, pp. 388–391. (1930).).

[40] H.-O. Kreiss and J. Lorenz. *Initial-boundary value problems and the Navier-Stokes equations*. Academic Press, Boston, 1989.

[41] B. S. Lazarov and O. Sigmund. Filters in topology optimization based on Helmholtz-type differential equations. *International Journal for Numerical Methods in Engineering*, 86(6):765–781, 2011.

[42] B. S. Lazarov and F. Wang. Maximum length scale in density based topology optimization. *Computer Methods in Applied Mechanics and Engineering*, 318:826–844, 2017.

[43] G. Legendre. *Rayonnement acoustique dans un fluide en écoulement: analyse mathématique et numérique de l'équation de Galbrun*. PhD thesis, ENSTA ParisTech, 2003.

[44] V. G. Maz'ja and T. O. Shaposhnikova. *Jacques Hadamard : a universal mathematician*. American Mathematical Society, Providence, 1998.

[45] M. Nagumo. Über eine Klasse der Mittelwerte. *Japanese Journal of Mathematics*, 7:71–79, 1930.

[46] J. Nečas. Sur une méthode pour résoudre les équations aux dérivées partielles du type elliptique, voisine de la variationnelle. *Annali della Scuola Normale Superiore di Pisa, Classe di Scienze*, 16(4):305–326, 1962.

[47] A. Pazy. *Semigroups of linear operators and applications to partial differential equations*, volume 44. Springer Science & Business Media, 2012.

[48] J. Petersson. Some convergence results in perimeter-controlled topology optimization. *Computer Methods in Applied Mechanics and Engineering*, 171:123–140, 1999.

[49] B. Poirée. Les équations de l'acoustique linéaire et non-linéaire dans un écoulement de fluide parfait. *Acta Acustica united with Acustica*, 57(1):5–25, 1985.

[50] J. Rauch. Symmetric positive systems with boundary characteristic of constant multiplicity. *Transactions of the American Mathematical Society*, 291(1):167–187, 1985.

[51] S. W. Rienstra and A. Hirschberg. An introduction to acoustics. Revised and updated version of reports IWDE 92-06 and IWDE 01-03, Eindhoven University of Technology, 2004.

[52] M. Schevenels and O. Sigmund. On the implementation and effectiveness of morphological close–open and open–close filters for topology optimization. *Structural and Multidisciplinary Optimization*, 54(1):15–21, 2016.

[53] O. Sigmund. Morphology-based black and white filters for topology optimization. *Structural and Multidisciplinary Optimization*, 33(4–5):401–424, 2007.

[54] O. Sigmund and A. Maute. Topology optimization approaches. *Structural and Multidisciplinary Optimization*, 48(6):1031–1055, 2013.

[55] M. Stolpe and K. Svanberg. On the trajectories of penalization methods for topology optimization. *Structural and Multidisciplinary Optimization*, 21(2):128–139, 2001.

[56] C. Sun. Moving average algorithms for diamond, hexagon, and general polygonal shaped window operations. *Pattern Recognition Letters*, 27(6):556–566, 2006.

[57] K. Svanberg. The method of moving asymptotes—a new method for structural optimization. *International Journal for Numerical Methods in Engineering*, 24(2):359–373, 1987.

[58] K. Svanberg. A class of globally convergent optimization methods based on conservative convex separable approximations. *SIAM Journal on Optimization*, 12(2):555–573, 2002.

[59] K. Svanberg and H. Svärd. Density filters for topology optimization based on the Pythagorean means. *Structural and Multidisciplinary Optimization*, 48(5):859–875, 2013.

[60] L. N. Trefethen and D. Bau. *Numerical linear algebra*. SIAM, Society for Industrial and Applied Mathematics, Philadelphia, 1997.

[61] F. Treyssède, G. Gabard, and M. Ben Tahar. A mixed finite element method for acoustic wave propagation in moving fluids based on an Eulerian–Lagrangian description. *The Journal of the Acoustical Society of America*, 113(2):705–716, 2003.

[62] F. Wang, B. S. Lazarov, and O. Sigmund. On projection methods, convergence and robust formulations in topology optimization. *Structural and Multidisciplinary Optimization*, 43(6):767–784, 2011.

[63] M. Y. Wang and S. Wang. Bilateral filtering for structural topology optimization. *International Journal for Numerical Methods in Engineering*, 63(13):1911–1938, 2005.